NO. DESSIN
DRAWING NO.

FORMAT ANSI B-11x17

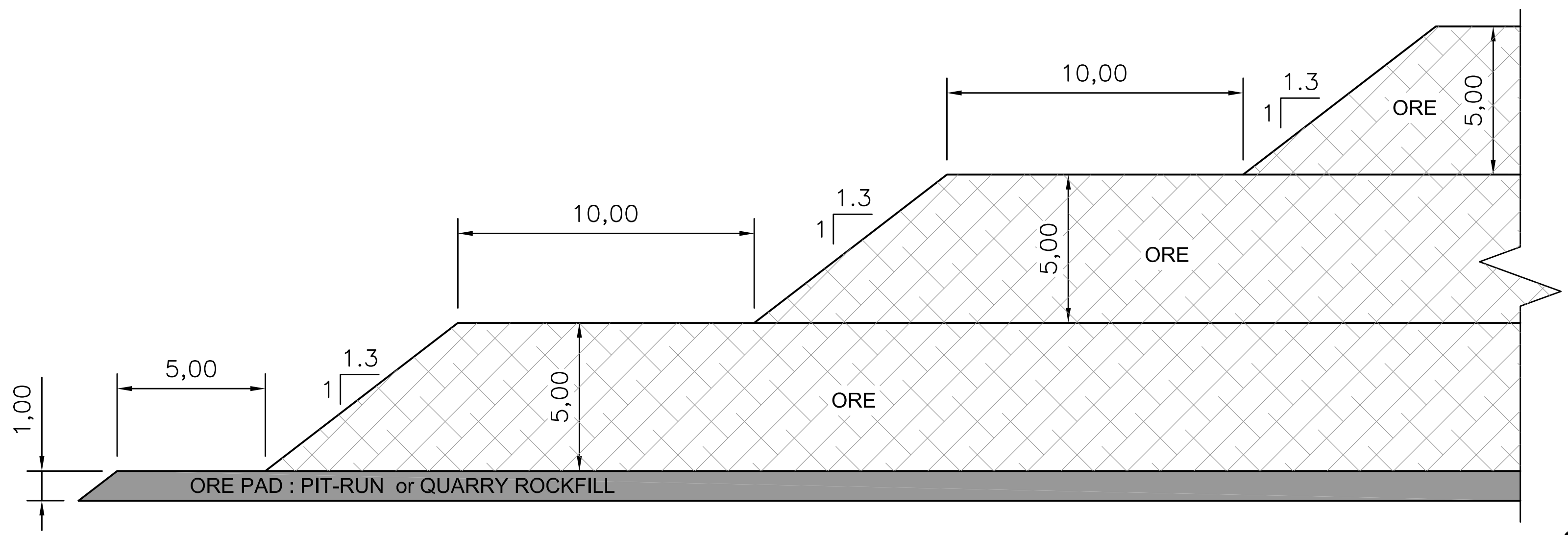

TYPICAL SECTION
SCL 1:250 (1H:1V)

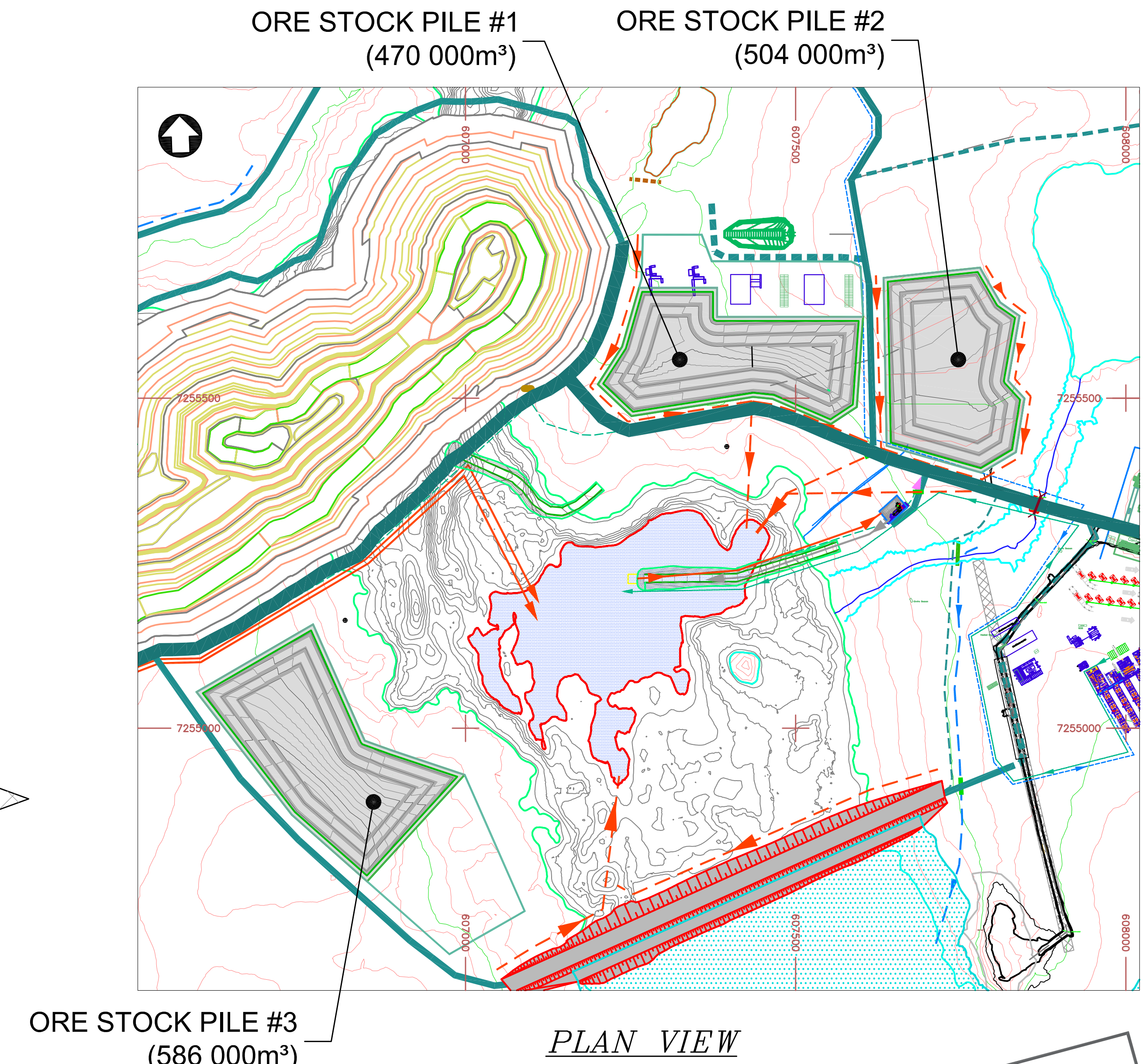

PLAN VIEW
SCL 1:10000

ISSUED FOR PERMITTING
DATE : 2016-05-03
AGNICO EAGLE

TITRE / TITLE	# DWG
–	–
–	–
–	–
–	–
–	–

DESSINS EN RÉFÉRENCE / REFERENCE DRAWINGS

REV	DESCRIPTION	DATE	PAR BY
0	ISSUED FOR PERMITTING	2016-05-03	J.C.

REVISIONS

AGNICO EAGLE
Golder Associates

DESSINÉ PAR / DRAWN BY	J.CRETE	DATE 2016-05-02
VÉRIFIÉ PAR / CHECKED BY	F.PETRUCCI	2016-05-03
APPROUVÉ PAR / APPROVED BY	S. OUELLET	2016-05-03
No. PROJET / PROJECT NO.	6108	
DATE	2016-05-02	

TITRE / TITLE
AGNICO-EAGLE – MEADOWBANK DIVISION
WHALE TAIL PIT PROJECT
ORE STOCK PILE #1, #2, #3
ORE PAD MAXIMUM CAPACITY
PLAN VIEW & TYPICAL SECTION

ÉCHELLE/ SCALE: A/S
FICHIER FILE: .DWG
No. DESSIN/ DRAWING NO.: 6108-687-210-001
REVISION: 0
FEUILLE/SHT: 1 / 1

AE-CART-ANSI B

N:\Projet\Amaruq\050 Studies\6108 Permitting Concepts\010 Info by area\687 Ore Stockpile\00 Drawings\6108-687-210-001_R0(OreStockPiles).dwg, 03 Mai 2016

Appendix B • TFSE Internal Structures Design

REPORT

April 19, 2018

MEADOWBANK TSF NORTH CELL

DETAILED ENGINEERING DESIGN OF INTERNAL STRUCTURE

Submitted to:
Patrice Gagnon
Alexandre Lavallée
Agnico Eagle Mines Limited
1957, 3rd Avenue West
Val-d'Or, Quebec
J9P 7B2

Report Number: 1784383 Rev. 0

Distribution:

1 hard copy - Agnico Eagle Mines Limited
1 e-copy - Agnico Eagle Mines Limited
1 e-copy - Golder Associates Ltd.

Golder Associates

Table of Contents

TABLES

FIGURES

APPENDICES

1.0 INTRODUCTION

Golder Associates Ltd. (Golder) has been retained by Agnico Eagle Mines Limited (AEM) to carry out detailed engineering design of internal structures for optimization of tailings deposition in the North Cell of the Tailings Storage Facility (TSF) at Meadowbank Mine, Nunavut.

The mine at Meadowbank has been in operation since the beginning of 2010. Tailings generated by the mine operation were deposited initially in the North Cell of the TSF, which was formed by dewatering the northwest arm of Second Portage Lake. The tailings deposition was completely transferred from the North Cell of the TSF to the South Cell in 2015.

AEM is planning to use the North Cell in 2019 to store tailings produced by milling of ore from the Amaruq Mine, located approximately 55 km north of the Meadowbank Mine. The intent of building internal structures within the North Cell is to allow for deposition of Amaruq tailings that, together with the internal dikes and rock cover, will establish the final landform defined for closure of the North Cell.

This report presents the design considerations and analyses, Design Drawings (Appendix A) and Technical Specifications (Appendix B) for the construction of the North Cell Internal Structure.

2.0 SITE BACKGROUND

2.1 Site Climate Data

The Meadowbank Mine is located at the southern limit of the Northern Arctic terrestrial ecozone, with a Low Arctic ecoclimate. This ecoregion is classified as a polar desert and is characterized by long cold winters and short cool summers. The Environment Canada meteorological station Baker Lake Airport (ID: 2300500), located about 84 km southwest from the site was selected to represent conditions at the Project site.

Daily precipitation and air temperature values are available from the Baker Lake A station for the period between 1946 and 2017 with some gaps. Additional climate data are available from an automatic weather station on site for the period between 2013 and 2017. The climate data set collected from the site weather station is short and therefore was not used for the statistical analyses presented below.

The average annual total precipitation at Baker Lake A station is 249 mm per year, with 59% precipitation falling as rain, and 41% falling as snow. Average annual lake evaporation was estimated to be 248 mm between June and September. The average annual loss of snowpack by sublimation is estimated as 72 mm between October and May. The annual average air temperature is -11.4°C and monthly average temperatures vary between -32.4°C in January and 12.1°C in July. A maximum daily temperature of 16.7°C has been recorded in the month of July and a minimum daily temperature of -35.8°C has been recorded in the month of January at the Baker Lake A station. The monthly average climate data for the Baker Lake A station are summarized in Table 1.

Winds are predominately from the northwest and exceed 20 kilometres per hour (km/hr) more than 25% of the time.

Table 1: Monthly Climatic Data Summary

Month	Average Temperature [1] (°C)	Rainfall [2] (mm)	Snowfall Water Equivalent [2] (mm)	Total Precipitation [2] (mm)	Lake Evaporation [2] (mm)	Snow Sublimation [2] (mm)
Jan	-32.4	0	7	7	0	9
Feb	-31.7	0	6	6	0	9
Mar	-26.3	0	9	9	0	9
Apr	-17.7	0	13	13	0	9
May	-6.3	5	8	13	0	9
Jun	3.7	18	3	21	9	0
Jul	12.1	39	0	39	99	0
Aug	9.7	42	1	43	100	0
Sep	3.4	35	7	42	40	0
Oct	-7.4	6	22	28	0	9
Nov	-17.9	0	17	17	0	9
Dec	-25.8	0	10	10	0	9
Total		**146**	**103**	**249**	**248**	**72**
Average	**-11.4**					

Notes:

1. Based on 1997-2004 Meadowbank Site data (Golder 2008a)
2. The Baker Lake A precipitation data were available between 1946 and 2015 (excluding years 1946-1949, 1973, 1993 and 2015). Smaller data gaps were filled using the average values from available years for the same day and month (SLI 2015)

2.2 Storm Events

24-hr duration rainfall values, representative of the Project are presented in Table 2, based on THE Intensity-duration-frequency (IDF) curves available from the Baker Lake A meteorological station (1987-2006) operated by Environment Canada (SLI 2015).

Table 2: Estimated Mine Site Extreme 24-hour Rainfall Events

Return Period (years)	24 hour Precipitation [1] (mm)
2	27
5	40
10	48
25	57
50	67
100	75
1000 [2]	101
PMP [3]	286

Notes:

1. Based on 1987-2006 Baker Lake A station Intensity-duration-frequency (IDF) curves (SLI, 2015)
2. IDF curve for return period higher than 100 years were computed based on the Gumble probability distribution and the method of moments (SLI, 2015).
3. PMP stands for Probable Maximum Precipitation and it is computed using the Hershfield formula based on the Baker Lake A annual IDF curves (SLI, 2015)

2.3 Rainfall Plus Snowmelt Events

Rainfall plus snowmelt values representative of the Project for durations between 1 day to 30 days and various return periods are presented in Table 3 below. These values are based on the Model 3 for western Canadian mountain basin model. These values were calculated by Environment Canada based on the IDF curves available from the Baker Lake A meteorological station (1950-2014).

Table 3: Mine Site Rain plus Snowmelt Events

Return Period (years)	Rain plus snowmelt [1] (mm)					
	1 day	5 day	10 day	15 day	20 day	30 day
2	19	59	86	98	104	108
5	27	80	118	133	143	149
10	32	93	139	156	169	176
25	39	111	166	186	202	211
50	44	123	186	208	227	236
100	49	136	206	230	251	262

Notes:

1. Based on 1950-2014 Baker Lake A station rain plus snowmelt Intensity-duration-frequency (IDF) curves

2.4 Site Seismicity

The Geological Survey of Canada (GSC) regularly evaluates regional seismic hazards and prepares seismic hazard maps based on statistical analysis of past earthquakes and also on knowledge of Canada's tectonics and geological structures. According to the 2015 Seismic Hazard Map prepared by GSC (2015), the mine site lies within a region of low seismicity. The peak horizontal ground accelerations (PGA) for Site Class C (average shear wave velocity 450 m/s) at various return periods are summarized in Table 4 for the Meadowbank Mine based on the 2015 National Building Code of Canada (NBCC) seismic hazard calculator (Appendix C).

Table 4: Site Peak Horizontal Ground Acceleration for Site Class C (NBCC, 2015)

Return Periods (Years)	1:100	1:500	1:1,000	1:2,500
Peak horizontal acceleration (g)	0.006	0.018	0.029	0.049

2.5 Permafrost

The Meadowbank Gold Project site is located within the zone of continuous permafrost. The land surface in the project area is underlain by continuous permafrost, while lakes that are deeper than about 2 m will be underlain by a talik, which is a zone of permanently unfrozen ground. Based on thermal studies carried out to date, the depth of permafrost is estimated to be on the order of 450 m to 550 m. The depth of the active layer ranges from about 1.3 m in areas with soils and up to about 4 m adjacent to lakes. The depth of permafrost and of the active layer will vary based on proximity to lakes, soils thickness, vegetation, climate conditions and slope direction.

Based on ground conductivity surveys and compilation of regional data, the ground ice content is expected to be low (0% to 10%). Ice lenses and ice wedges are locally present on land, as indicated by ground conductivity, and by permafrost features such as palsas. These areas of local ground ice are generally associated with low lying areas of poor drainage.

Lake ice thicknesses of between 1.5 m and 2.5 m have been encountered during geotechnical investigations in mid to late spring. It is possible that mid-winter ice thickness will be greater; however, no data relating to ice thickness currently exists for the mid-winter period.

Ground temperatures have been monitored at Baker Lake since 1997 as part of the Circumpolar Active Layer Monitoring (CALM) program. The mean annual ground temperature at an estimated depth of 2 m for the Baker Lake CALM station ranges between -6.6 °C and -8.4 °C.

3.0 TAILINGS STORAGE FACILITY (TSF)

3.1 TSF Arrangement

The mine at Meadowbank has been in operation since the beginning of 2010. Tailings generated by the mine operation are deposited in the basin formed by dewatering the northwest arm of Second Portage Lake. The TSF dikes are built around and across the basin, and include:

- The Central Dike;
- The Stormwater Dike (SWD); and
- Saddle Dams.

The Central Dike and Saddle Dams are permanent structures. The SWD separates tailings management in the north basin (North Cell) and water management in the south basin (South Cell).

3.2 North Cell Dikes

The typical dike section includes a rockfill with a 3 horizontal (H): 1 vertical (V) upstream face with bituminous geomembrane liner, filters, and cut-off trench. The main characteristics of the North Cell dikes are presented in Table 5. Construction materials are primarily generated from materials on site.

Table 5: Main Characteristics of the North Cell Dikes

Dike	Crest Elevation (masl)	Maximum Height at Rockfill Crest Center Line (m)	Rockfill Width at Crest (m)	Crest Length (m)	Maximum Base Width (m)
Stormwater Dike	150	22	10	1070	105
Saddle Dam 1	150	16	10	380	80
Saddle Dam 2	150	8	10	485	50

Notes:
1. Max. base width shown for rockfill only.
2. Saddle Dams have upstream slopes of 3H: 1V and downstream slopes of 1.5H: 1 V.
3. The SWD has an upstream slope of 3H: 1V, and downstream slopes at angle of repose.

3.3 Meadowbank Tailings Deposition Plan

Prior to start-up, a deposition plan for the TSF was developed in 2009. This deposition plan was based on assumptions such as:

- The construction sequence planned for the dikes;
- The in-situ dry density (assumed to be 1.31 t/m^3);
- The volume loss due to ice build-up (estimated at 20% for the purpose of the study and included in the assumed in-situ dry density);
- The percentage solids of the tailings (around 45%);
- The production rate (8,500 tons per day with a ramp up from 60% to 100% of production rate within 4 months); and
- The slopes of tailings beaches of 1% above water and 5% below water.

As of February 2010, tailings were deposited in the North Cell of the TSF, as the South cell was not operational at that time. Golder updated the deposition plan for the next two years of operation between 2011 and 2012 with tailings being deposited primarily in the North Cell. Since 2012, AEM has developed the deposition plan for the TSF.

Since 2014, the tailings have been deposited in the North Cell and South Cell in two phases, as described below (AEM, 2015):

- **Phase 1**
  - North Cell: July 2014 to November 2014; and
  - South Cell: November 2014 to June 2015.
- **Phase 2**
  - North Cell: July 2015 to October 2015; and
  - South Cell: October 2015-July 2018.

Based on this, the North Cell has not been receiving any tailings since October 2015. The current maximum tailings surface elevation in the North Cell is 149.5 m.

3.4 Amaruq Tailings Deposition Plan

Based on a preliminary deposition plan developed by AEM, the North Cell Internal Structure raise would allow the deposition of an additional 3,294,000 t (2,111,538 m^3) tailings processed from the Amaruq ore between the years 2019 to 2021 AEM (2017a). AEM's preliminary deposition plan was developed using the following assumptions:

- The average (nominal) mill throughput will be 9,000 t /day;
- The average expected tailings dry density in the North Cell is 1.56 t/m^3;

- The North Cell will receive tailings only four months in a year (1,098,000 t/year or 703,846 m^3/year) during the summer months between June and September;
- The ice entrapment at the North Cell is expected to be zero as tailings deposition will only take place during summer months; and
- During winter months, the tailings will be deposited into the South Cell.

It is understood that the deposition plan will be updated by AEM once the North Cell Internal Structure design has been completed.

3.5 Geotechnical Information

3.5.1 Site Investigations

Original ground conditions beneath the North Cell basin and the North Cell dikes are available from extensive borehole investigations performed in 2002 and 2009. The borehole locations are presented in Appendix A (Drawing 003).

Another geotechnical investigation program was carried out by AEM in 2014 aimed to gain additional knowledge on the tailings material and on its frozen state. The program included 12 diamond drill holes, two test pit excavations and the installation of 2 thermistors all located within the North Tailings Cell (North Cell), mainly in the area upstream of Saddle Dams 1 and 2 (Area A) and upstream of the SWD (Area B). The selected borehole locations were all within the tailings away from the upstream toes of the dikes and dams. The north section of the North Cell was not investigated as very little or no tailings had been deposited at the time in the area. The Records of Boreholes for this investigation are presented in Appendix B.

Additional geotechnical investigation was carried out by Golder (2017a) to gather more information on the SWD current subsurface condition. The program included drilling of three boreholes, installing three thermistors and installing vibrating wire piezometers. One of the boreholes (SWD-01-17) was drilled through the frozen tailings in the North Cell while the other two were drilled through the stability berm at the toe of the SWD in the South Cell. The tailings samples obtained from SWD-01-17 were used to characterize the in-situ geotechnical properties of the existing tailings in this study. The Records of Boreholes for this investigation are presented in Appendix D.

3.5.2 In situ Tailings Condition

Based upon the geotechnical investigations and the available topographic mapping, the tailings have an approximate thickness ranging from 3 m to 24 m. The 2017 borehole (SWD-01-17) indicates that the tailings are partially to completely frozen to an approximate depth of 17 m (i.e. bottom of tailings at the location of SWD-01-17), with some intercalated zones of thawed and frozen tailings.

3.5.3 Natural Ground Conditions

The stratigraphy beneath the deposited tailings generally consists of a 3.8 m average thickness of lake bed sediments which overlay a 2 m average thickness of glacial deposits in the form of till. Extensive laboratory testing has been completed on the till and lake bed sediments during previous design and construction stages of the Meadowbank project. The relevant existing borehole locations are presented in Appendix A (Drawing 003).

The bedrock is composed mainly of ultramafic and mafic sequences and metasedimentary rocks. Extensive laboratory (UCS, Young's modulus, durability, etc.) and in-situ (hydraulic conductivity) testing have been completed on the bedrock in this area.

3.6 Tailings Properties

3.6.1 Existing Tailings

3.6.1.1 Laboratory Testing Results

A series of laboratory tests was carried out on tailings samples in connection with the current study. Tailings samples obtained previously from borehole SDW-01-17 were shipped to the Golder geotechnical laboratory in Calgary for testing. The testing included: particle size analysis (sieve and laser method), thaw consolidation test (frozen tailings), confined and unconfined compressive strength (frozen tailings), compressive creep test (frozen tailings), and thermal conductivity (frozen and unfrozen). The details of laboratory testing carried out on the existing tailings in this study are presented in Appendix E.

Figure 1 shows the particle size distribution of tailings samples tested in this study (SDW-01-17, RC1, RC5, RC7, RC8 and RC10). The tailings mostly comprise silt-sized particles (i.e. less than 0.075 mm based on the Unified Soil Classification System), with between 95% and 75% passing the 0.075-mm sieve, and 19% or less particles smaller than 0.005 mm. The D_{10}, D_{30}, and D_{60} have been estimated as 0.0039 mm, 0.012 mm, and 0.0336 mm for tailings.

Thermal analyses of the tailings were carried on frozen and unfrozen tailings samples. The average thermal conductivity ranges from 1.983 W/m°C to 3.336 W/m°C for tailings at 10 and -5 degrees Celsius, respectively. A summary of thermal conductivity for two tailings samples tested in this study is presented in Table 6.

Table 6: Thermal Conductivity of Existing Tailings.

<table>
<tr><th rowspan="2">Sample</th><th rowspan="2">Water Content (%)</th><th rowspan="2">Void Ratio</th><th rowspan="2">Porosity (%)</th><th rowspan="2">Saturation (%)</th><th colspan="6">Avg. Thermal Conductivity, (W/m°C)</th></tr>
<tr><th colspan="4">Frozen</th><th colspan="2">Unfrozen</th></tr>
<tr><td rowspan="2">SDW-01-17 (RC5)</td><td rowspan="2">31.7</td><td rowspan="2">1.1</td><td rowspan="2">51.43</td><td rowspan="2">89.8</td><td colspan="4">At -5 °C</td><td colspan="2">At 10 °C</td></tr>
<tr><td colspan="4">3.336</td><td colspan="2">1.983</td></tr>
<tr><td rowspan="2">SDW-01-17 (RC10)</td><td rowspan="2">31.7</td><td rowspan="2">1.0</td><td rowspan="2">50.27</td><td rowspan="2">94.1</td><td>-2°C</td><td>-1.5°C</td><td>-1°C</td><td>-0.5°C</td><td>3.7°C</td><td>10°C</td></tr>
<tr><td>3.36</td><td>4.93</td><td>7.56</td><td>2.45</td><td>2.343</td><td>2.453</td></tr>
<tr><td colspan="5" rowspan="2">Average between RC5 and RC10</td><td colspan="4">Between -2 °C and -5 °C</td><td colspan="2">At 10 °C</td></tr>
<tr><td colspan="4">3.348</td><td colspan="2">2.218</td></tr>
</table>

A peak frozen unconfined compressive strength (UCS) of 414 kPa was measured at -3 °C for sample SDW-01-17–RC1. In contrast, a peak frozen Confined Compressive Strength of 812 kPa was measured at -3 °C for sample SDW-01-17– RC10 at confining stress of 350 kPa. The compressive creep test results on the frozen tailings sample SDW-01-17–RC1 at -3 °C indicated strain rates of 0.1 %/day, 2.6 %/day and 40.7 %/day at loading stages of 50 kPa, 150 kPa and 350 kPa, respectively. Results of thaw-consolidation performed on samples RC-7 and RC-9 for a 50-kPa stress showed total axial strain of 24.6 and 8.4%, respectively.

The implications associated with tailings creep and thaw-consolidation, and the potential effect on the stability of the Internal Structure will be discussed in Section 5.4.

3.6.1.2 Previously Reported Geotechnical Properties

As summarized in Golder (2017a), the specific gravity of the Meadowbank Mine tailings ranges from 2.97 to 3.03. The hydraulic conductivity has been estimated to range from 3 x 10^{-5} m/s to 7.6 x 10^{-9} m/s. A mix of tailings samples tested in 2008 resulted in maximum Standard Proctor dry density of 1715 kg/m^3. A soil-water characteristic curve (SWCC) was measured for a sample of mixed tailings that showed an air entry value (i.e. the suction at which the sample starts to desaturate, AEV) of about 25 kPa. Thermal analyses of the tailings were previously carried out by Golder (2008a) and RIME UQAT-Polytechnique which resulted in a thermal conductivity for a 77.5% saturation ranging from 1.98 W/m°C to 3.21 W/m°C for tailings at 16 and -18 degrees Celsius, respectively.

3.6.2 Amaruq Tailings

A series of geotechnical laboratory testing has been performed by Golder (2017c) on the Amaruq tailings to define geotechnical properties including: particle size distribution (PSD), specific gravity, hydraulic conductivity, thermal conductivity, consolidation behaviour, soil water characteristic curve (SWCC) and shrinkage curve. The details of laboratory testing are presented in Appendix E.

The PSD of Amaruq tailings was determined by using a mechanical sieving and hydrometer as well as Fritsch laser particle size analyzer. Figure 1 presents the PSD curve for the tailings sample tested using a mechanical sieving and hydrometer. It is apparent that the Amaruq tailings curve is close to the fine gradation limit of the existing tailings. The specific gravity values for Amaruq tailings ranged from 2.91 to 2.96.

The hydraulic conductivity of Amaruq tailings at standard temperature was 1.23 10^{-5} cm/s, 8.01 10^{-6} cm/s, and 6.30 10^{-6} cm/s at effective consolidation stress of 100 kPa, 300 kPa, and 600 kPa, respectively.

The coefficient of consolidation (c_v) of Amaruq tailings ranged from 0.18 to 4.55 (cm^2/s) under various pressures. A Standard Proctor test was conducted on Amaruq tailings. The maximum dry density of the tailings was 1,880 kg/m^3 with an optimum moisture content of 12.6%. The corresponding wet density was 2,117 kg/m^3.

The thermal conductivity was carried out using Decagon device KD2 Pro compliant on an Amaruq tailings slurry (Whale Tails - 106µm Tailings) having a water content of 30.5%. Average thermal conductivity at room temperature was 1.805 W/m°C, and measured value at -13.6°C was 3.017 W/m°C.

The soil water characteristics curve was also obtained for Amaruq tailings and the shrinkage limit was measured to be 19% with a minimum void ratio of 0.56.

3.7 Instrumentation Data

Instrumentation installed in the North Cell includes: thermistors, vibrating wire piezometers, and extensometers. Information records of about 14 thermistors strings (installed between 2012 and 2017) are available. Some of these thermistors were lost during deposition, but their historical data can still be of use.

Temperature profiles obtained from the thermistor strings NC17-1 to NC17-8, and SDW17-1 indicate a clear trend for the tailings to freeze back, but tailings at the location of several thermistors (e.g. NC17-2, NC17-3, NC17-8 and SDW17-1) show that the lower portion of the tailings body is still thawed. Other thermistors strings (e.g. NC17-1, NC14-4, NC17-5, NC17-6 and NC17-7) show that the mid-portion of the tailings body is within a near-zero temperature, where water and ice can coexist, or even water only, depending on the salinity and freezing point of tailings water. In general, the thermistors show that the upper 3 to 10 m of tailings are frozen, except for the first 1 to 2 m which is located within the active zone and therefore subject to seasonal freeze and thaw cycles.

Temperature profiles obtained from the thermistor strings at Saddle Dam 1 (T1) also indicate that the entire body of tailings are frozen, except for the first 1 to 2 m located within the active zone subject to freeze and thaw cycles. The temperature profiles for the rockfill dam and natural ground were also obtained from thermistor strings at Saddle Dam 1 (T2, T3 and T4).

Two experimental insulation covers were tested at the Meadowbank Mine site to assess the performance of insulation covers on the tailings storage facility (Awoh et al., 2016). Both covers consisted of inert waste rock, with one being 2 m thick and the other being 4 m thick. On each experimental cell, volumetric water content, matric suction and temperature sensors were installed at three stations and at various depths. The results suggest that in the 4 m cell, the tailings remain below the freezing point all year long, while in the 2 m cell, the temperatures at the tailings-waste rock interface rise seasonally to very close to the freezing point (0 to 0.5 ° C). These results were consistent with the data obtained from the thermistor Rock Fill-1-2 (73-6) where the tailings covered with 3.5 m waste rock remained frozen all year long.

The information obtained from the thermistors strings was considered sufficient to support the different design analyses and were used to define frozen and thawed zones within the tailings, as well as existing tailings temperature. Some key thermistor data are presented in Appendix F.

4.0 DESIGN BASIS CRITERIA

4.1 North Cell Dam Hazard Classification

The Canadian Dam Association (CDA) developed Dam Safety Guidelines (CDA, 2014). These guidelines provide design criteria for establishing hazard potential classification, Inflow Design Flood (IDF), and Earthquake Design Ground Motion (EDGM) for the design of dams.

The guidelines provide recommendations on the classification of dams with respect to the consequences associated with a presumed dam failure. These consequences are to be evaluated in terms of incremental consequences over and above the consequences of the given event if the dam failure had not occurred. The guidelines recommend that the incremental consequences of a dam failure should be evaluated in terms of:

- Loss of life;
- Property losses;
- Environmental losses; and
- Cultural or built Heritage losses.

A hazard potential classification of “Significant” was selected based on the above-mentioned categories for the Internal Structure of North Cell, mainly based on the assumption that there will be a temporary impact on the fish habitat of Third Portage Lake if Saddle Dams 1 and 2 fail along with the North Cell Internal Structure.

4.2 Seismic Design Parameters

CDA (2014) recommends that dams with a "Significant" hazard classification to have to meet the following two EDGM criteria:

- Operation: between 1 in 100 and 1 in 1,000 year return peak horizontal acceleration; and
- Passive Closure: 1 in 2,500-year return peak horizontal acceleration.

Golder used the passive closure EDGM for the design, which corresponds to a PGA of 0.049g based on the 2015 NBCC seismic hazard calculator (Table 4).

4.3 Design Flood

CDA (2014) recommends that dams with a "Significant" hazard classification meet the following two IDF criteria:

- Operation: between the 1 in 100 and 1 in 1,000 year return period flood; and
- Passive Closure: 1/3 between the 1,000-year return period flood and the probable maximum flood (PMF).

Golder used the operational IDF for the design of ditches at the toe of the North Cell Internal Structure.

4.4 Dam Stability

Table 7 presents the minimum factors of safety (FOS) for slope stability of the North Cell Internal Structure to be adopted during design based on the CDA (2014) guidelines.

Table 7: Factors of Safety for Slope Stability (CDA, 2014)

Loading Condition	Minimum Factor of Safety
Short-term (immediately after construction)	1.3
Long-term steady state (once the facility is operating)	1.5
Pseudo-static	1.0
Post-earthquake	1.2

5.0 DETAILED DESIGN

The design considered all aspects of constructability including seasonal supply of materials, construction season and schedule, stability, thermal effects, deformation, seepage and resistance to external and internal erosion forces.

5.1 Internal Structure Design

5.1.1 Methodology and Alignment

The Internal Structure will be constructed within the footprint limit of the North Cell on the upstream side of the existing Saddle Dams and the North Cell perimeters, as presented in Drawing 002 (Appendix A). The Internal Structure alignment was designed to maximize tailings storage and to meet closure requirements while ensuring long-term stability as well as retaining the tailings and allowing seepage to flow through, as explained in the following paragraphs and subsections.

The ultimate crest elevation of 154 masl for the Internal Structure has been selected based on the required storage capacity. The crest elevation of the North Cell Internal Structure was designed to be 154 m for the most part. Near the SWD, the crest elevation of the North Cell Internal Structure will taper from 154 m to 150 m. At this location, sufficient space was provided at the downstream to allow the Internal Structure to be raised to elevation 154 m should this become necessary due to a change in the tailings deposition plan.

The Internal Structure was designed to be founded on the existing tailings. The construction of the Internal Structure was expected to be carried out in one stage during winter when the tailings foundation remains frozen.

An offset was considered from the downstream toe of the Internal Structure to the crest of existing Saddle Dam or the perimeter of the North Cell. The purpose of the offset was to allow for seepage collection. The offset varies depending on the existing configuration of the North Cell (e.g., existing rockfill platforms) and minimum working area or seepage control requirement, while the maximum offset of 15 m was considered on the upstream side of Saddle Dam 1. It was understood that AEM might construct a 2 m rockfill platform closure cover on the upstream side of the North Cell, which might affect the ditch construction and stability of the Internal Structure.

To collect seepage and contact runoffs, temporary ditches and sumps will be provided between the footprint limit of the North Cell and the downstream toe of the North Cell Internal Structure. The details of the ditch and sump designs are described in Section 5.5.

5.1.2 Design Cross-section

The Internal Structure crest width depends on:

- Roadway requirements;
- Constructability; and
- Requirement to operate the tailings pipeline on the crest of the Internal Structure.

Minimum rockfill crest width was set at 30.0 m including the width for safety berms which are required on haul roads. The minimum height of the safety berms is 2.3 m.

The upstream (interior) side slope of the Internal Structure was set to be 3H:1V for long term stability and constructability of the filter layers.

The downstream (exterior) side slope of Internal Structure was determined based on the results of the thermal, seepage and slope stability analyses. As presented in Drawing 002 (Appendix A), the downstream side slope varies from 1.5H:1V to 2.5H:1V depending on the foundation conditions. The results of the thermal, seepage and slope stability analyses are described in Section 5.4.

As presented in Drawing 012 (Appendix A), the North Cell Internal Structure generally consists of three material zones:

1- Zone 1: main portion of the Internal Structure using Non-Potential Acid Generating (NPAG) Run-of Mine waste rock;
2- Zone 2: Coarse filter on the upstream side slope to provide compatibility between the Zone 1 and Zone 3 materials; and
3- Zone 3: Fine filter on the upstream slope over Zone 2 using screened or crushed waste rock compatible with the tailings.

The internal Structure will be used to contain the tailings and also to provide a platform to discharge the tailings from. At tailings discharge points, an extra 5 m wide strip of erosion protection (i.e., 0.5 m thick coarse filter) or a geomembrane liner is required. In addition, an extra erosion protection layer (i.e., 0.5 m thick coarse filter) may be required at the locations where the Internal Structure is exposed to the tailings pond.

Sections 5.2 and 5.3 discuss the filter compatibility and material properties of the zones, respectively.

5.2 Filter Compatibility

The filter design criteria published by Sherard and Dunnigan (1989) were used to design the grain-size distribution (gradation) of granular filters needed to prevent tailings from moving into (internal erosion or piping) the Internal Structure and to ensure adequate drainage.

1) Criteria:

- For particle retention are summarized in the table below.

Group	Base Soil Description	
	Percent Finer than 0.08 mm	**Filter Criteria**
1	Less than 15%	$D_{15} \leq 4\ to\ 5\ \times\ d_{85}$
2	15 % to 39 %	$D_{15} \leq \left(\frac{40 - A}{40 - 15}\right) \times \left((4 \times D_{85}) - 0.7\ mm\right) + 0.7$
3	40% to 85%	$D_{15} \leq 0.7\ mm$
4	More than 85%	$D_{15} \leq 9\ \times\ d_{85}$

Where "A" = percentage passing sieve 0.08 mm

"D" represents the filter material and "d" the material to be protected

- To ensure adequate drainage
  $D_{15}/d_{15} > 5$

Note: The dimension d_{85} should be derived from the grain size curve of the fraction of material passing the 5 mm sieve.

2) The percentage of particles in the filter passing the 0.08 mm sieve shall be less than 5 %.
3) The largest particle size in the filter shall be less than 80 mm.

In addition:

- The coefficient of uniformity (D_{60}/D_{10}) for the filter material shall not exceed 20 to limit segregation potential; and
- The fines content shall be non-plastic.

The criteria for the elements within the Internal Structure section also include:

- Constructability – must be able to efficiently construct in cold or freezing conditions to meet the construction schedule; and

- Must be able to function in a very cold environment without degradation.

For the purpose of filter compatibility, the PSD curve for the Amaruq tailings presented in Figure 1 was used. The tailings are categorized as Group 3 and meet all 3 above mentioned criteria. However, the proposed gradations for the fine filter exceed the maximum coefficient of uniformity defined as CU = D_{60}/D_{10} (i.e., equal or less than 6). In this case, a special care is required during placement of the filter materials to avoid segregation. Two filter zones made of fine and coarse crushed NPAG waste rock are proposed based on the criteria, as presented in Figure 2.

5.2.1.1 Coarse Filter

The Coarse Filter is designed to prevent movement of Fine Filter material into the rockfill. The Coarse Filter was designed based on the above-mentioned criteria and on gradations of materials produced based on the method suggested in Section 5.3. Gradation limits for the Coarse Filter are presented in Figure 2 and listed in both Table 8 and in the Technical Specifications in Appendix B.

Table 8: Recommended Coarse Filter Gradation for the Internal Structure

Size (mm)	%Passing	%Passing
200		100
152		86
76	100	42
25	52	14
12.7	35	10
4.76	23	5
2	15	3
0.425	10	1
0.075	7	0

5.2.1.2 Fine Filter

The Fine Filter gradation is designed to prevent tailings from moving into the Coarse Filter. Gradation limits for the Fine Filter are presented in Figure 2 and listed in both Table 9 and in the Technical Specifications in Appendix B.

Table 9: Recommended Fine Filter Gradation for the Internal Structure

Size (mm)	%Passing	%Passing
38.1		100
19.05		65
12.7	100	50
4.76	60	28
2	40	16
0.425	23	6
0.075	10	0

5.3 Construction Materials

The bulk of the North Cell Internal Structure is planned to be constructed using NPAG Run-of Mine waste rock with an upstream side slope covered with filter zones using screened or crushed NPAG rock compatible with the tailings.

5.3.1 Run-off Mine NPAG Waste Rock (Rockfill)

In general, the NPAG waste rock material is reported to include grain sizes varying from silt-sized particles to boulders up to 2 m in diameter. The grain-size distribution of the NPAG waste rock was measured from a blast design fragmentation prediction in 2008. The specific gravity for the NPAG waste rock was determined to be approximately 2.90. Some unconfined compressive strength (UCS) and direct shear tests were performed on the NPAG core resulting in an average UCS of 80 MPa. The peak internal friction angle results from direct shear tests are not conclusive and resulted in average peak friction angle of 47 degrees.

5.3.2 Crushed and Screened NPAG Waste Rock (Filter)

Crushed and screened NPAG rockfill results in grain size curves which vary widely, with fines content ranging from 0% to 10% and cobbles ranging from 0% to 40%. The hydraulic conductivity also depends heavily on the screening performed with material passing the 50 mm and 20 mm screens resulting in hydraulic conductivities of 7.9×10^{-2} cm/s to 1.6×10^{-5} cm/s, respectively. Thermal conductivity analyses were also performed on the fraction passing 20 mm resulting in a thermal conductivity ranging from 2.2 W/mºC to 3.75 W/mºC; depending upon the starting temperature and degree of saturation.

Drained, strain-controlled triaxial tests were also completed on screened NPAG rockfill (passing 16 mm) resulting in a range of internal friction angles of 31 to 34 degrees. The crushed NPAG rockfill was also tested for mass loss due to freeze thaw cycles. The preliminary results show mass loss to be less than 7.8% depending on the grain size fractions considered.

5.4 Design Analysis

To evaluate the potential impact of thaw consolidation on the integrity and stability of the North Cell Internal Structure, a coupled seepage/thermal model and slope stability analysis were recommended by the Meadowbank Review Board.

Two representative cross sections of the North Cell incorporating both the Internal Structure geometry and the underlying tailings were used for the models, as follows:

- Cross-section 1 (CH 0+825) was selected at the location of the Saddle Dam; and
- Cross-section 2 (CH 1+465) was selected on the east end of the North Cell where a 2 m rockfill layer has already been placed.

5.4.1 Methodology

5.4.1.1 Coupled Seepage/Thermal Model

The coupled seepage/thermal models were prepared using the finite element codes TEMP/W and SEEP/W, developed by Geo-Slope International Ltd. (2007). The thermal model incorporated water percolating through the Internal Structure, computed concomitantly in the seepage model, with the associated convective heat transfer. The seepage component of the model included an infiltration rate of 80% of total precipitation as the model top boundary condition over the Internal Structure, and also considered a constant water table at elevation of 153.5 m within freshly deposited tailings. A ground temperature function was assigned as the top boundary for the thermal model. Initial model conditions were derived based on field instrumentation. The freezing point of water was defined as -0.5°C based on results of salinity and thermal conductivity tests as presented in Appendix E.

The ultimate objective of the model was to assess whether the tailings underneath the Internal Structure could thaw over time and the extent to which the thaw front could advance. If the tailings remain frozen, infiltrating water would flow laterally through the permeable rockfill through the Internal Structure over the top of the frozen tailings. If the tailings underneath the rockfill raise were to thaw, this could lead to an increase in pore-water pressures in the tailings that could potentially impact the integrity and stability of the dike. The coupled seepage/thermal model was performed at different stages based on the proposed construction of the Internal Structure and Amaruq tailings deposition plan, as summarized in Table 10. Thermal modeling was completed in three steps and convective thermal/seepage modeling was completed in one step, as follows:

Stage 1: a thermal steady state analysis was performed to generate initial thermal conditions required for the subsequent transient models based on the ground temperature observed from thermistors data in November. In this stage, the Internal Structure was not included in the model geometry.

Stage 2: an initial transient analysis was performed to determine temporal variation in ground temperature from November to June (210 days), with the Internal Structure included in the model geometry. The model top boundary condition included an estimated ground temperature function generated from a 6-year climate dataset (Golder, 2008a), which is consistent with the climate dataset obtained from Baker Lake A Station (1950-2016). The average ground temperature function is presented on Figure 3.

Stage 3: a subsequent transient analysis was run including freshly deposited tailings in the model geometry. The purpose was to assess the impact of warm freshly deposited tailings on temperatures within the Internal Structure and existing tailings from June to November of the second year (210 to 730 days). The ground temperature function shown in Figure 3 was used as model top boundary conditions, and a constant temperature of -5°C was adopted as lower boundary condition for the model. The tailings temperature at the time of deposition was considered to be 15°C.

Stage 4: a separate transient coupled convective heat transfer thermal/seepage analysis was also performed to assess the impact of seepage on the heat transfer within the Internal Structure and existing tailings from June to November of the second year (210 to 730 days). The model geometry includes the Internal Structure and freshly deposited tailings. For the thermal component in the transient convective heat transfer thermal/seepage analysis, the ground temperature function shown in Figure 3 was used as model top boundary condition, and a constant temperature of -5°C was adopted as lower boundary condition for the model. The tailings temperature at the time of deposition was considered to be 15°C. For the seepage component in the transient convective heat transfer thermal/seepage analysis, an initial condition was defined based on a steady state seepage analysis. Downstream boundary conditions included a pressure head equal to zero to simulate a drain at the downstream toe of the Internal Structure for Section 1 and a review boundary to simulate drainage at the ditch for Section 2. A constant infiltration rate of 1.1 mm/day was also considered as the top rockfill boundary condition in the analysis, corresponding to 80% of total precipitation (Table 3) rate in 6 month (From June to November).

Table 10: The Coupled Seepage/Thermal Model Summary

Model Stage	Geometry	Model	Start/ End	Boundary Condition / Initial Condition	Parent Analysis	Reference
Stage 1	2017 tailings surface	Steady State/ Thermal	November 1^{st}	Initial ground temperature based on thermistor data (November data)	NA	Thermistor T1, T3 and T4 for cross-section 1 Thermistor Rock Fill-1-2 (73-6) and field experiment results for cross-section 2
Stage 2	Constructed Internal Structure (154 masl) on the 2017 tailings surface	Transient/ Thermal	November 1^{st} /May 30^{th}	Ground surface temperature variation with time	Stage 1	Ground surface function Figure 3 based on Golder (2008a)
Stage 3	Amaruq Tailings surface at its ultimate elevation with the Internal Structure (153.5 masl)	Transient/ Thermal	June 1^{st} / November 1^{st}, plus additional Year (i.e., November of the second year)	Ground surface temperature variation with time	Stage 2	Ground surface function Figure 3 based on Golder (2008a)
Stage 4	Amaruq Tailings surface at its ultimate elevation with the Internal Structure (153.5 masl)	Convective Heat Transfer/Thermal Component	June 1^{st} / November 1^{st}, plus additional Year (i.e., November of the second year)	Ground surface temperature variation with time	Stage 2	Ground surface function Figure 3 based on Golder (2008a)
		Convective Heat Transfer/Seepage Component		Infiltration / Steady State		80% of total precipitation presented in Table 3

5.4.1.2 Slope Stability Model

Stability analyses were performed using the GeoStudio 2007 SLOPE/W, Version 7.17 computer program for general solution of slope stability by two-dimensional limit equilibrium methods. Slope stability analysis was conducted using the same cross sections defined for the coupled thermal/seepage models to evaluate the FOS of the ultimate geometry of the Internal Structure to ensure that FOS values meet the criteria defined for closure conditions. The selected method of analysis was the Morgenstern-Price Method with a half-sine function to model the inter-slice forces.

A range of potential slip surfaces was analysed for the different scenarios including thawed foundation using undrained and effective stress shear strength parameters, and for static and pseudo-static analyses, as summarized in Table 11

Table 11: Stability Analysis Model Summary

Geometry	Type of Analysis	Parent Analysis
Cross-section 1 Amaruq Tailings surface at its ultimate elevation with the Internal Structure (154 masl)	Static (Undrained for portions of thawed tailings based on the results of thermal models)	Piezometric water level based on the seepage analysis
	Static (Effective Stress Analysis)	
	Pseudo-static (Undrained Analysis for portions of thawed tailings)	
Cross-section 2 Amaruq Tailings surface at its ultimate elevation with the Internal Structure (154 masl)	Static (Undrained for portions of thawed tailings)	Piezometric water level based on the seepage analysis
	Static (Effective Stress Analysis)	
	Pseudo-static (Undrained parameters for thawed tailings)	

5.4.2 Material Properties

5.4.2.1 Thermal Parameters

Table 12 presents material properties used for thermal analyses. The thermal properties of tailings were defined based on results of laboratory tests on the existing and Amaruq tailings, as described in Section 3.6.

The thermal conductivity of the other materials was primarily defined based on the Johansen equation (Johansen, 1975), as well as reported values from the literature (Geoslope 2004, Nidal H, 2000 and MEND 1998). The volumetric heat capacity of the materials was estimated based on the method proposed by Johnston et al. (1981).

Estimates of the unfrozen water content relationship with temperature were made for the tailings and foundation materials using the relationship presented by Anderson et al. (1973) and published parameters for similar materials from Nixon (1991).

Table 12: Material Properties for Thermal Analysis

Material	Dry Density (t/m^3)	Specific Gravity, Gs (t/m^3)	Porosity, n (%)	Initial Volumetric Water Content [(1)]	Thermal Conductivity (W/m°C)		Volumetric Heat Capacity ($MJ/m^3{}^oC$)	
					Frozen	Unfrozen	Frozen	Unfrozen
Tailings	1.492	3.0	50.27	0.51	3.348	2.218	2.1	2.759
Rockfill saturated	2.15	3.2	32.8	0.328	2.6	1.8	2.2	2.9
Rockfill unsaturated	2.15	3.2	32.8	0.02	0.75	0.75	1.0	1.0
Filter	1.9	2.89	34.3	0.095	2.0	1.4	1.6	1.8
Till	1.87	2.71	31.0	0.31	2.4	1.8	2.0	2.6
Bedrock	2.71	3.0	-	0.005	2.9	2.9	2.5	2.5

(1) Variation in the degree of saturation and volumetric water contents at different time steps are obtained from the Seepage component of the model. The thermal conductivity and volumetric heat capacity are then adjusted by the TEMP/W solver.

(2) The tailings are expected to consolidate with time and reach an average void ratio of 1.0 or less. Sizing of the impoundment was made considering progressive tailings consolidation and allowance was made for ice entrapment.

5.4.2.2 Hydraulic Properties

The values of hydraulic conductivity used for seepage analyses are summarized in Table 13. In addition to the saturated hydraulic conductivity, the soil water characteristics curves (SWCC) and hydraulic conductivity functions for tailings and rockfill were used in this study, as presented in Appendix H.

Table 13: Material Properties for Seepage Analysis

Material	Saturated Hydraulic Conductivity (m/s)			K ratio Khorizontal Kvertical	Reference
	Minimum Observed Values	Maximum Observed Values	Analyses		
Till	$7x10^{-8}$	$2x10^{-4}$	$1x10^{-7}$	1	Falling head tests from 2002, Section 4.4.2
Rockfill and Filters (NPAG run-of-mine)	-	-	$1x10^{-3}$	1	Experience with similar materials. Golder (2017b)
Upper Bedrock	$2x10^{-7}$	$5x10^{-5}$	$5x10^{-6}$	1	2003 and 2006 investigations[a,b,c]
Lower Bedrock	$3x10^{-9}$	10^{-6}	$2x10^{-7}$	1	2002, 2003 and 2006 investigations[a,b,c]
Tailings	$3x10^{-5}$	$7.6x10^{-9}$	1×10^{-7}	1	Previous 2002 and 2003 geotechnical field investigations. Golder (2017b)
Bituminous Geomembrane Liner			Impermeable [d]		See Note [d]

[a]Golder 2003c Appendix II, [b]Golder 2006d Appendix III, [c]No discernable difference in hydraulic conductivity of the various rock types. The hydraulic conductivity appears to vary with depth. The hydraulic conductivity of shallow exfoliated and weathered bedrock, regardless of rock type, is generally higher than the deeper less fractured rock, [d]Seepage through the bituminous geomembrane liner was estimated as a constant rate of 100 L/ha/day based on average rates reported for liners in landfill applications (Bonaparte et al. 2002).

5.4.2.3 Shear Strength Parameters

The material properties used for stability analysis are listed in Table 14.

Table 14: Material Properties for Slope Stability Analysis

Material	Bulk Unit Weight (kN/m^3)	Effective Stress Parameters		Undrained Strength Su (kPa) or Shear Strnegth Rario	Reference
		Cohesion, c (kPa)	Angle of Internal Friction (°)		
Compacted Rockfill (NPAG run-of-mine)	22	0	38	Not Applicable	Golder (2017b)
Fine and Coarse Filters (crushed NPAG waste rock)	19.8	0	38	Not Applicable	Golder (2017b)
Till	21.4	0	32	-	
Tailings (thawed)	18.0	0	30	0.15	Assume range of strength values

Material	Bulk Unit Weight (kN/m^3)	Effective Stress Parameters		Undrained Strength Su (kPa) or Shear Strnegth Rario	Reference
		Cohesion, c (kPa)	Angle of Internal Friction (º)		
Frozen Tailings (lower than -3°C)	18.0	400	-	-	Lab Results, Appendix E
Frozen Tailings (between 0 and -3°C)	18.0	200	-	-	Assumed
Bedrock	n/a	n/a	n/a	n/a	Assumed impenetrable

For pseudo-static conditions a coefficient of horizontal acceleration of 0.049g (corresponding to a predicted 1 in 2,500 year event) was applied.

5.4.3 Analyses Results

5.4.3.1 Thermal Analysis Results

The Internal Structure is designed to operate in seasonally frozen and unfrozen conditions. The variation of active zone depth at the toe of Cross-sections 1 and 2 is illustrated in Figures 4 and 5, respectively, for a complete year after deposition of Amaruq tailings based on the thermal component of the convective heat transfer analysis results (i.e., Stage 4).

The thermal analyses indicate that the 5 m high Internal Structure will protect most of its tailings foundation from thawing all year round. However, some sections of the exposed existing tailings downstream of the Internal Structure, as shown on Cross-section 1, will undergo freeze and thaw cycles. The active zone in these sections is predicted to be about 2.5 m to 3.5 m deep. In addition, the tailings foundation will undergo freeze and thaw cycles where the thickness of the sloping rockfill is less than 2 m.

For the sections where a 2 m rockfill is already in place (i.e., Cross-section 2), the depth of active zone depends on the thickness of the previously placed rockfill (i.e., varies with an average of 2 m) and the location of the downstream ditch. The active zone in these sections are predicted to be about 2.5 m below the ground surface. It is apparent that the maximum depth of thaw occurs in September.

The details of thermal analysis results for Stages 1, 2 and 4, as described in Table 10, are presented in Figures G-1 to G-6 in Appendix G.

A comparison between the thermal model (Stage 3) and the thermal component of the convective heat transfer model (Stage 4, where water flow is considered) shows that the heat transfer associated with seepage may result in thawing of a greater area in comparison with results of the thermal model only, with no effect of seepage (Stage 3). Generally, the active zone based on the results of the thermal component of the convective heat transfer model (Stage 4) is greater than those of the thermal model only (Stage 3). For instance, Figures 6 and 7 illustrate the effect of seepage on the depth of active zone and thermal profile at the toes of Cross-sections 1 and 2 respectively for the month of September.

Results of the coupled seepage/thermal models indicate that the portion of tailings foundation underneath the dyke that would thaw during summer will be restricted to a zone near the downstream toe of the dyke, and that the effect of seepage will not cause this zone to change much compared to thermal-only model results.

5.4.3.2 Seepage Analysis Results

The Internal Structure was modelled to predict seepage rates for use in sizing of seepage collection systems. It was observed that seepage rates through the Internal Structure associated with the deposition of fresh tailings are not significant compared to storm design parameters. Predicted seepage flux rates for the Internal Structure at two cross-sections are presented in Table 15. The variation of flux rate versus time for each representative cross-section is presented in Figures 8 and 9.

Modeled cross-sections for Stages 4 and 6 showing typical predicted water table locations and contours of total hydraulic head are presented in Figures H-1- to H-5 in Appendix H.

Table 15: Summary of Predicted Seepage Rates

Cross-section	Month of Maximum Flux Rate	Flux Rate at the Downstream Toe of Internal Structure (m^3/day/m)	Flux Rate through the Internal Structure (m^3/day/m)
1	September	0.196	0.116
2	August	0.0021	0.0015

For the sections similar to Cross-section 1(CH 0+825), the seepage will be collected between the downstream toe of the Internal Structure and the Saddle Dam without construction of a ditch. The details of seepage collection management are described in Section 5.5.

For the sections similar to Cross-section 2, the seepage cannot be collected completely by the proposed ditch, which is mainly designed to convey the storm event (see Section 5.5). In this case, it is anticipated that the maximum amount of seepage will pass through a section beneath the proposed ditch in August (Table 15). Based on the thermal analysis (Figure H-4), the permafrost is at a minimum elevation of 148.1 masl at this location (i.e., beneath the ditch) while the maximum elevation of the permafrost at the downstream is estimated to be 149.8 masl. Considering the maximum flux rate of 0.0021 m^3/days, the cross-section area below the ditch (i.e., ~1 m^2) will receive the seepage with a rate of 2.43×10^{-8} m/s, which is significantly lower than the saturated permeability of the materials (tailings or till 1×10^{-7} m/s) in this area. This suggests that the seepage can be stored naturally in this area without reporting to the existing intact water collection ditch around the perimeter of the North Cell.

5.4.3.3 Stability Analysis Results

The stability analyses were performed based on the results of thermal analyses considering the worst-case scenario in terms of the biggest area of the active zone (i.e., in September). Based on this, the tailings area was divided into three different zones:

1- Thawed zones for tailings with temperature higher than -0.5°C;

2- Frozen tailings with temperature between -0.5°C and -3°C; and

3- Frozen tailings with temperature lower than -3°C.

In the undrained analysis, the undrained shear strength parameters were used for tailings while effective stress parameters were used in the effective stress analysis, as summarized in Table 14.

Results of stability analyses for Cross-sections 1 and 2 are summarized in Table 16 and illustrated in Figures I-1 to I-6 in Appendix I. All slopes meet the minimum FOS requirement based on the proposed downstream slope of the Internal Structure.

Table 16: Stability Analysis Results Summary

Cross-section	Type of Analysis	Downstream Slope	FOS		Minimum Requirement (CDA, 2017)	Figure
			Undrained Analysis	Effective Stress Analysis		
1	Static	2.5H:1V	1.5	1.7	1.5	I-1 and I-2
	Pseudo-static		1.3	N/A	1.0	I-3
2	Static	1.5H:1V	2.3	2.6	1.5	I-4 and I-5
	Pseudo-static		2.1	N/A	1.0	I-6

Note that the tailings against the upstream slope stabilize the Internal Structure against upstream failure modes.

5.4.4 Considerations on Creep and Thaw-Consolidation

Compressive Creep and Thaw-Consolidation tests were conducted in the laboratory on undisturbed samples of frozen tailings obtained from borehole SWD-17-01. Details of these tests are presented in Appendix E.

5.4.4.1 Tailings Creeping

A Compressive Creep test was performed on sample RC7, collected from between 8.75 and 10.25 m below the tailings surface, and with the presence of ice lens indicated in the borehole log. The test was performed for compressive axial stresses of 50, 150 and 350 kPa, and the sample was kept at constant temperature of -3^{o}C during the test. The sample was undisturbed, and despite the fact of being collected from an average depth of 9.5 m below the tailings surface, it presented dry density of about 890 kg/m^3 and 77% water content, reflecting the presence of entrapped ice. Therefore, results of creep tests on such a loose sample are expected to apply for portions of tailings with high ice content.

The creep test for each loading stage ran until a constant creep strain rate was established. The rest results indicated creep rates of 0.1%/day for a 50 kPa load, 2.6%/day for 150 kPa load, and as high as 40.7%/day for the maximum applied load of 350 kPa. The test results suggest that tailings at the Meadowbank site could experience significant creep in portions with high ice content and low density. The extent of creep on site will however depend on the spatial distribution of ice lens within the tailings body, depth, internal temperature conditions, and additional loading applied to the tailings.

The Internal Structure will have maximum height of about 5 m, meaning an additional load of approximately 110 kPa on top of the tailings surface. If loose portions of tailings containing ice lens exist at lower depths beneath the Internal Structure, creep could occur. Due to uncertainties associated with location of ice lens within the North Cell in general, and underneath the footprint of the new Internal Structure specifically, it is not possible to determine the potential extent of creep upon construction of the Internal Structure. Instrumentation is recommended in Section 5.6 to monitor deformations underneath the Internal Structure, and further evaluation of creep trends should be conducted once field data is available.

5.4.4.2 Thaw-Consolidation

Thaw-consolidation tests were performed on test specimens obtained from frozen undisturbed tailings core samples RC7 and RC9. Core RC7 was extracted between 8.75 m and 10.25 m below the tailings surface and reported to contain ice lens. RC9 was obtained from between 11.75 m and 13.25 m below the tailings surface, and not reported to contain ice lenses.

The test consisted of setting the frozen test specimen onto a load frame and applying a 40 kPa load on top of the sample (equivalent to about 1.9 m of rockfill). The load frame was then moved to a separate location in the laboratory at room temperature to allow the sample to thaw, with consolidation (axial strain) during the thawing process being monitored.

Sample RC7 had an initial dry density of 1,165 kg/m^3 and a gravimetric moisture content of about 56%, reflecting the initial loose state of the sample associated with ice entrapment. Sample RC7 experienced a total axial strain of 24.6%. Sample RC9 did not contain visible ice entrapment and had a higher initial dry density of 1,494 kg/m^3 and a 31% moisture content. Sample RC9 experienced a measured axial strain of about 8.2%.

The first aspect that could be associated with thaw-consolidation is the possible generation of excess pore-water pressures in the tailings in the event that thawing occurs faster than tailings drainage. This aspect was assessed in the stability analysis presented in Section 5.4.3.1. The results of stability analysis considering tailings at undrained conditions showed there should be no instability for the Internal Structure constructed with the design downstream slopes.

Another aspect associated with thaw-consolidation is differential displacement. The tests showed that axial strain between 8 and 25% could occur upon thawing of tailings under the dyke toe. The thermal models presented in Section 5.4.3 showed that tailings underneath the Internal Structure would not thaw, except for a limited portion under the toe, where the rockfill thickness will not be enough to insulate the tailings against the active thaw zone. Therefore, only that limited portion of tailings under the Internal Structure toe would be subject to freeze/thaw cycles and prone to thaw-consolidation.

Assuming that tailings under the dyke toe could thaw down to 1.5 m below the tailings surface (i.e. 1 m of rockfill on top of tailings with a 2.5 m deep active zone) and considering the range of thaw consolidation measured in the laboratory, potential tailings consolidation could be between 0.12 to 0.38 m, in the worst-case scenario with tailings containing high ice entrapment. This range of consolidation at the toe of the dyke would not cause the dyke to fail but could lead to the appearance of cracks associated with differential displacement at the toe and under the dyke crest.

Visual inspection should be conducted during summer time to assess whether thaw-consolidation is, in fact, occurring and whether the development of cracks is expected. If cracks are observed at the toe of the Internal Structure, additional rockfill should be placed as required.

5.5 Ditch and Sump Design

A total of seven (7) perimeter ditches have been designed around the Internal Structure to handle flows from the 25-yr 24-hour rainfall event (57 mm) and convey runoff into four (4) sumps to be excavated below the ground surface. The purpose of the perimeter ditches and sumps is to collect runoff from the downstream face of the Internal Structure and surrounding areas and to collect toe seepage for pumping into the internal pond as required. Based on the seepage modelling results provided in Table 15 in Section 5.4.3.2, the seepage rates reporting at the toe of Internal Structures are approximately 2 orders of magnitude lower than the peak runoff flows under the design event and therefore seepage is considered negligible for the sump/pump design calculations.

The following ditches were designed parallel to the internal structures:

- Ditch 1 collects runoff from a catchment area of 2.3 ha at the southwest corner of the Internal Structures and drains southwest for approximately 367 m into Sump 1.
- Ditch 2a collects runoff from a catchment area of 5.1 ha from the mid-west area the Internal Structures and drains northwest for approximately 238 m into Sump 2.
- Ditch 2b collects runoff from a catchment area of 2.7 ha at the northwest corner of the Internal Structures and drains south for approximately 585 m into Sump 2.
- Ditch 3a collects runoff from a catchment area of 2.5 ha at the northwest corner of the Internal Structures and drains east for approximately 315 m into Sump 3.
- Ditch 3b collects runoff from a catchment area of 7.9 ha at the northwest corner of the Internal Structures and drains west for approximately 560 m into Sump 3.
- Ditch 4a collects runoff from a catchment area of 10.1 ha at the east side of the Internal Structures including drainage from an existing waste rock facility and drains south for approximately 537 m into Sump 4.
- Ditch 4b collects runoff from a catchment area of 13.3 ha at the southwest corner of the Internal Structures including drainage from an existing waste rock facility and drains north for approximately 397 m into Sump 4.

The sumps and the respective pumping systems discussed below are designed with the assumption that the Internal Structure and the surrounding waste rock dumps are at a breakthrough moisture content. It is Golder's understanding that AEM is currently observing on site much lower flow rates than those that are predicted in Table 18. This indicates that the waste rock structures on site have not yet reached to their "breakthrough moisture content". Under the circumstances, AEM could decide to install smaller capacity pumps that are sized to meet observed flows, with the prospect that it may become necessary to increase the pump sizes later if and when the seepage flows increase.

Due to space limitations, no ditches or sumps were designed along the west side of the Internal Structure (adjacent to Saddle Dam 1). At this location, Ditch 2a will be extended through a rock cut to convey runoff accumulated against the Internal Structure. It has been assumed that a small residual pond will be formed, and that pumping will occasionally be required following large storm/rainfall plus snowmelt events.

For sizing the active storage for the sumps, a comparison was carried out of a combination of various pumping rates, volumes and storm events (5-day 25-yr rainfall plus snowmelt event and 25-yr 24-hr rainfall storm event). The results of the analysis determined that it was impracticable to provide the sump volume required to store the entire 5-day 25-yr rainfall plus snowmelt event due to space limitations and large storage requirements. Based on a trade-off between sump sizing and pumping rates, it was decided to size the sumps for the 25-yr 24-hr rainfall storm event with higher peak flows. At the same time, the recommended pumps have enough capacity to handle the 5-day 25-yr rainfall plus snowmelt assuming semi-continuous operation throughout the event.

The routing of the both the 24 hour and 5 day storm event were modeled using HEC-HMS, hydrologic software developed by the U.S. Army Corps of Engineers (USACE, 2015). The catchment areas presented are the total catchment areas for each of the ditches, while the lag time is the based on the travel time for the longest flow path through the perimeter ditch to the downstream sump.

Losses along the flow path were simulated using the SCS Curve Number (CN). A high CN value of 94 was assumed for the sizing, assuming that the summer storm event could occur during the snowmelt period when the ground is still highly saturated. The use of this CN value effectively ignores the time lag effects whereby rock fill material can store runoff and release it slowly over time. This approach is conservative because it assumes that rainfall peaks result in nearly instantaneous runoff from both runoff and interflow (i.e. flow which infiltrates into the rock fill and reports later as toe seepage).

The frequency storm method was selected for the distribution of the 24-hr rainfall storm event. Short-term IDF curves for the Baker Lake A station were used to produce the 24-hr synthetic storm with a peak intensity of 12.5 mm/hr.

The alternating blocks method was selected to develop the 5-day rainfall plus snowmelt event. Rainfall plus snowmelt IDF curves for the Baker Lake A station were used to produce the 5-day synthetic storm with a peak intensity of 18.3 mm/day or 0.8 mm/hr intensity.

Based on the peak flows from the hydrological model, the hydraulic capacity of the ditches was determined using Manning's Equation (Chow, 1973). The following parameters were used in the design calculations:

- Manning's n: 0.022 (typical for channels excavated in rockfill) or 0.035 (typical for lined channel or channels overlain with filtered granular material);
- Ditch side slopes: 2H:1V for stability;
- Ditch bottom width of 1.0 m; and
- Minimum ditch depth of 0.5 m.

The calculated water depth and flow velocity in the ditches under the design storm event are summarized in Table 17.

Table 17: Ditch Sizing results

Catchment	Catchment Area (ha)	Bed Slope (%)	Flow Depth (m)	Peak Flow (m^3/s)	Peak Velocity (m/s)
Ditch 1	2.3	0.3	0.13	0.08	0.5
Ditch 2a[1]	5.1	0.9	0.18	0.25	1.0
Ditch 2b[1]	2.7	0.7	0.16	0.17	0.8
Ditch 3a	2.5	0.3	0.21	0.13	0.5
Ditch 3b	7.9	0.3	0.36	0.35	0.6
Ditch 4a	10.1	0.3	0.40	0.46	0.6
Ditch 4b[3]	13.3	0.3	0.54	0.74	1.7

Note: [1] Lined channel with 0.5 m thick fine filtered granular material

[2] Excavated channel on tailings overlain with 0.3 m thick fine filtered granular material

[3] Minimum ditch depth of 1.0 m to allow a minimum freeboard of 0.2 m

The sumps downstream of the ditches have been sized to handle flows from storm events. The 25-yr 24-hr rainfall storm event was selected as the design event. The same model used to size the perimeter ditches was used to size the sumps.

The sump size is a trade-off between sump volume and pump size. Following optimization in the model, the resulting sump size, volume and peak pumping rates are shown in Table 18. As with the perimeter ditches, seepage rates from the internal structures were not included in the assessment because they are much smaller than the runoff volumes.

For the sump sizing it has been assumed that the sumps will be emptied every year before the winter and therefore no ice build-up losses over the winter were accounted for. A dead storage of 0.5 m was considered for the operation of the pumps. The sumps will be excavated below ground surface with side slopes of 3H:1V and a total depth of 4 m.

Table 18. Sump Size Results

Sump		Sump 1	Sump 2	Sump 3	Sump 4[2]
Sump Base Surface Area (m^2)		9	100	225	396
Sump Top Surface Area (m^2)		729	1,156	1,521	1,225
Sump Active Volume[1] (m^3)		756	1,533	2,268	1,203
Peak Pumping Rate	(m^3/hr)	15	150	150	1,400
	(L/s)	4.2	42	42	389
5-day 25-yr Rain plus snowmelt Storm	Inflow Volume (m^3)	2,110	7,260	9,640	21,770
	Peak Inflow (L/s)	10	34	45	101
	Peak Elevation (m)	3.4	0.5	0.9	0.50
	Freeboard (m)	0.1	3.0	2.6	2.5
24-hour 25-yr Rainfall Storm	Inflow Volume (m^3)	900	3,360	4,460	10,080
	Peak Inflow (L/s)	80	419	471	1,163
	Peak Elevation (m)	3.4	3.2	3.4	2.9
	Freeboard (m)	0.1	0.3	0.1	0.1
Recommended Pumping Rate	(m^3/hr)	25	150	150	1,400
	(USGPM)	110	660	660	6,160

[1] The actual sump volume does not take into consideration a 0.5 m of dead storage at the bottom of the sump and 0.5 m to 1 m of dead storage at the top for the ditches inlets.

[2] Maximum possible peak elevation of 3.0 m to allow for a 1 m of dead storage at the top for the 1.0 m deep ditch inlets.

As presented in Table 18, the selected pumping rates are capable of handling the rain plus snowmelt volumes assuming a constant pumping rate throughout the storm.

As discussed above, the sumps and the respective pumping systems are designed with the assumption that the Internal Structure and the surrounding waste rock dumps are at a breakthrough moisture content. If AEM chooses, the pumping systems can be staged by using lower rates and increase pump sizes later if needed based on the field observations.

5.6 Instrumentation

Upon construction of the dyke, instrumentation should be installed to allow for monitoring of temperature, displacements and deformation within the Internal Structure and tailings underneath. Data from the instrumentation program will provide the means to evaluate the processes of tailings freeze-back, creep and thaw-consolidation. The following instrumentation is recommended:

a) Thermistors strings installed through the Internal Structure and tailings underneath. Thermistors should be installed at the main section of the Internal Structure adjacent to Saddle Dams 1 and 2, as well as at two additional locations east and west of the dyke main section.
b) Survey monuments placed on the crest and downstream face of the Internal Structure. These will allow for the monitoring of settlements and the evaluation of whether differential displacements are occurring associated with thaw-consolidation of tailings under the dyke's toe.

5.7 Bill of Quantities

The quantities of materials required for the construction of the Internal Structure, ditches and sumps were estimated based on the Drawings in Appendix A. The material quantities table for the internal structures, ditches and sumps are presented in Appendix J.

6.0 CONSTRUCTION CONSIDERATIONS

The Internal Structure, ditches and sumps shall be constructed following the Technical Specifications (Appendix B).

The construction schedule for the Internal Structure needs to be timed according to the season. In particular, the placement of the Zone 1 fill should take place in the late winter, after the underlying thawed tailings have had a chance to re-freeze. This will facilitate equipment trafficability and will also provide a more favorable thermal regime in the foundations (consistent with the assumptions in the thermal modeling). On the other hand, the placement of the upstream filter layers will have to be undertaken in spring, summer or fall so that the materials can be properly placed and compacted in an unfrozen state.

Construction tasks for the Internal Structure will include (not listed in order):

- Foundation preparation including snow removal;
- Placement of Zone 1 fill (selected NPAG waste rock) including compaction by a smooth drum compactor with a minimum of 4 passes. The upstream face of the Internal Structure shall be re-sloped after placement. The material shall be placed in lifts not exceeding 2 m in thickness;
- Preparation of stockpiles of coarse and fine filter materials;
- Filter placement and compaction by vibratory roller;
- Installation of instrumentation; and
- Construction of seepage collection works.

Seepage collection ditches and sumps will be excavated into the existing tailings or rockfill downstream of the Internal Structure. Excavation can be completed during foundation preparation or later during operations.

Report Signature Page

GOLDER ASSOCIATES LTD.

Reza Moghaddam, Ph.D., P.Eng.
Geotechnical Engineer

Adriana Parada, M.Eng., P.Eng
Water Resources Engineer

Kebreab Habte, M.Sc., P.Eng.
Senior Geotechnical Engineer

Fernando Junqueira, M.Sc., Ph.D., P.Eng.
Senior Geotechnical Engineer

Ken Bocking, M.Sc., P.Eng
Principal

AP/RM/KH/FJ/KAB/sk

https://golderassociates.sharepoint.com/sites/16157g/proposal project management/project/9 - phases 3000 4000 det eng desgn&rprtg/design report_final/1784383_north cell internal dike raise - design report_rev0_19apr2018.docx

REFERENCES

Agnico Eagle Mines Limited (2014). Tailings Storage Facility Investigation Program – Meadowbank Gold Project, July 2014.

Agnico Eagle Mines Limited (2017a). Deposition Plan – TSFE Amaruq Deposition Plan (9000tpd) V1.

Agnico Eagle Mines Limited (2017b). Meadowbank Mine Site Weather Station data (2013-2017).

Agnico Eagle Mines Limited (2017c). North Cell, TSF, and planned closure topographic mapping – Delivered as AutoCAD files (Final closure cover.dxf).

Agnico Eagle Mines Limited (2017d). North Cell, TSF, contour maps 2014-2017– Delivered as AutoCAD files (major contours of SurfaceNC 2017.dxf, NC_final_Oct2015 (backward analysis).dwg, and NC (November 2014) End of Phase 1.dwg)

Agnico Eagle Mines Limited (2017e). Diversion Ditches As-built and Limit for North Cell Internal Structure – Delivered as AutoCAD files (DivDitch_Contours_0_5m_UTM.dwg, and 4 TO 1 Slope from diversion ditch - crest limit for internal structure.dxf)

Agnico Eagle Mines Limited (2017f). Water balance - Amaruq_9000tpd-1.

Anderson, D., Tice, A., and McKim, H., 1973. The Unfrozen Water Content and the Apparent Heat Capacity in Frozen Soils. Proceedings, 2nd International permafrost conference, Yakutsk, pp289- 295.

Awoh, S.A., Bussière, B., Batzenschlager, C., Boulanger-Martel, V., Lepine, Voyer, E. (2016). Design, construction and preliminary results of two insulation covers at the Meadowbank Mine. Geo-Chicago 2016, August 14-18, 2016.

Bonaparte, R., Daniel, D.E., and Koerner, R.M. 2002. Assessment Recommendations for Improving the Performance of Waste Containment Systems. US EPA Doc. EPA/600/R-02/099. December.

Canadian Dam Association (CDA), 2014. Technical Bulletin: Application of Dam Safety Guidelines to Mining Dams.

Chow, Ven Te (1973). Open-Channel Hydraulics.

GEOSLOPE Ltd (2007). Thermal Modeling with TEMP/W. An Engineering Methodology. TEMP/W User Manual. Calgary, May 2007.

Golder Associates Ltd. (2003a). Field Geotechnical Studies Meadowbank Project Nunavut.

Golder Associates Ltd. (2003b). Permafrost Thermal Regime Baseline Studies, Meadowbank Project Nunavut. Report. Golder Associates Ltd. December 2003.

Golder Associates Ltd. (2007). Winter 2006 Second Portage Tailings Dike Geotechnical Drilling Hydrogeological, and Televiewer Investigations, Meadowbank Gold project, Nunavut. Report. Golder Associates Ltd. January 25, 2007.

Golder Associates Ltd. (2008a). Coupled Thermal/Seepage and Containment Transport Modeling for the Tailings Facility, Meadowbank Gold Project.

Golder Associates Ltd. (2008b). Tailings Storage Facility Dike Design, Meadowbank Gold Project.

Golder Associates Ltd. (2017a). Geotechnical Field Investigation and Performance Assessment, Stormwater Dike, Meadowbank Gold Project.

Golder Associates Ltd. (2017b). North Cell Internal Structure – Data Gap analysis and Design Criteria Meadowbank Mine.

Golder Associates Ltd. (2017c). Laboratory Testing on Tailings, Whale Tail Pit Project.

Johansen, G.H., Ladanyi. B., Morgenstem, N.R., and Penner, E. (1981). Engineering Characteristics of Frozen and Thawing Soils. Permafrost Engineering Design and Construction. Edited by John Wiley & Sons.

Johansen, O. 1975. Thermal Conductivity of Soils. Ph. D. Diss, Norwegian Technical Univ., Trondheim; also, U.S Army Cold Reg. Res. Eng. Lab Transl. 637, July 1977.

MEND (1998). Acid Mine Drainage Behaviour in Low Temperature Regimes. Thermal Properties of Tailings. MEND Project 1.62.2. July 1998.

Nidal H. et al (2000), Soil Thermal Conductivity. Effects of Density, Moisture, Salt Concentration and Organic Matter Soil Science Society of America Journal 64:1285-1290 (2000)

Nixon, J.F. (1991) Discrete Ice Lens Theory for Frost Heave in Soils, Canadian Geotechnical Journal, Volume 28, 843-859.

O'Kane Consultants Inc. (2015). TSF North Cell Closure Design Report Construction Plan, Prepared for Agnico Eagle Mines Limited – Meadowbank Mine, 948/1-02, November 2015.

O'Kane Consultants Inc. (2016). Meadowbank North Cell TSF Expansion—Design of Internal Structures, Prepared for Agnico Eagle Mines Limited – Meadowbank Mine, 948/2-01, March 2016.

Sabrina Lord (2013). RIME UQAT-Polytechnique – Caracterisations des Materiaux Pouvant Etre Utilises Pour des Recouvrements Miniers en Milieu Nordique – Mine Meadowbank.

SNC Lavalin (SLI) (2015). Whale Tail Pit Project – Permitting Level Engineering. Geotechnical and Water Management Infrastructure. Dated November 12, 2015. Report No. 6108-REP-004_RA.

Vincent Boulanger-Martel, et al. (September 2017). Meadowbank's TSF Experimental Cells: RIME's Research Program.

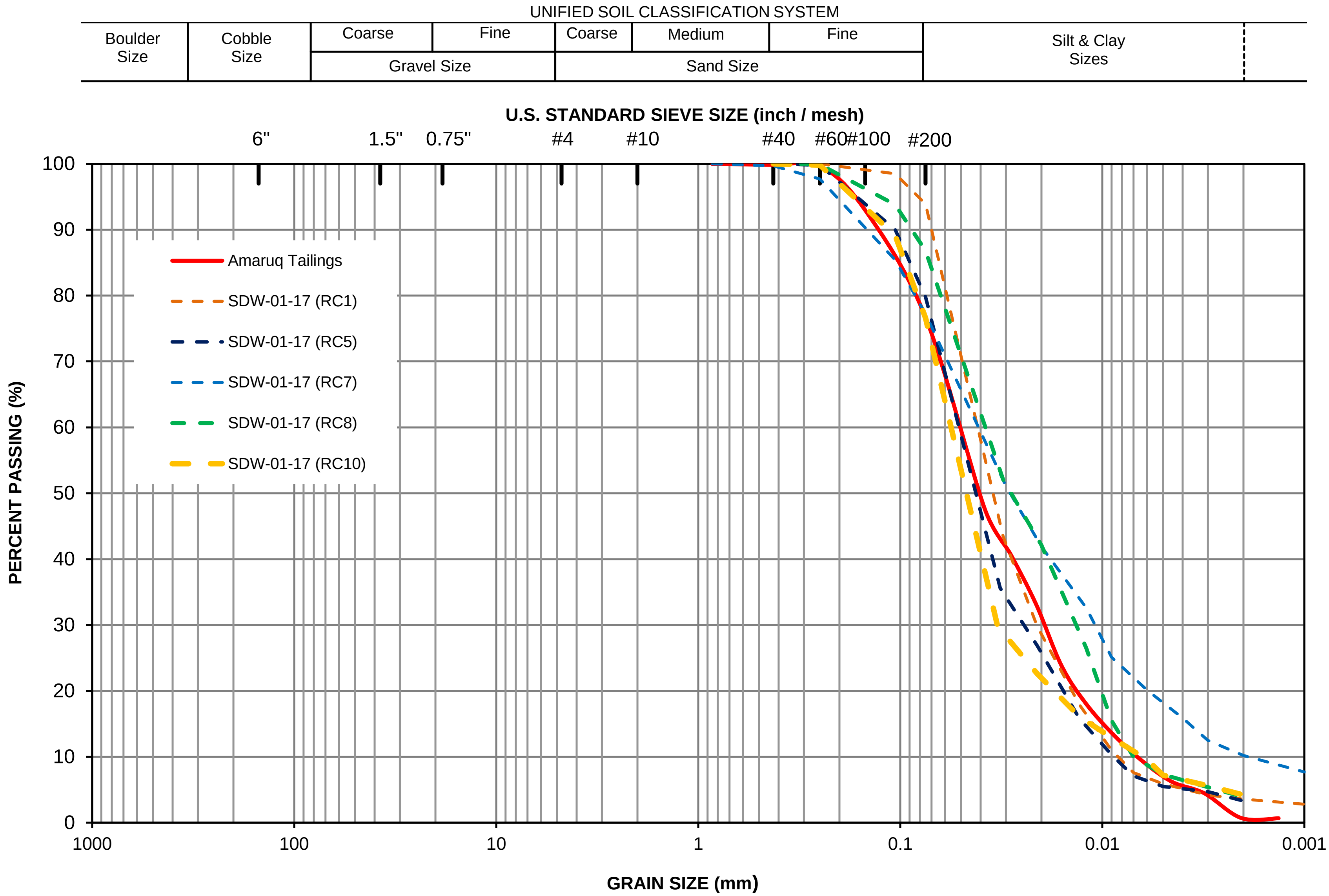

CLIENT **AEM**	PROJECT **Meadowbank North Cell TSF Design**

CONSULTANT

Golder Associates

YYYY-MM-DD	2016-05-27
DESIGNED	RM
PREPARED	RM
REVIEWED	KH
APPROVED	KAB

TITLE

TAILINGS PARTICLE SIZE DISTRIBUTIONS

TITLE	PHASE	REV	FIGURE
1784383		**0**	**1**

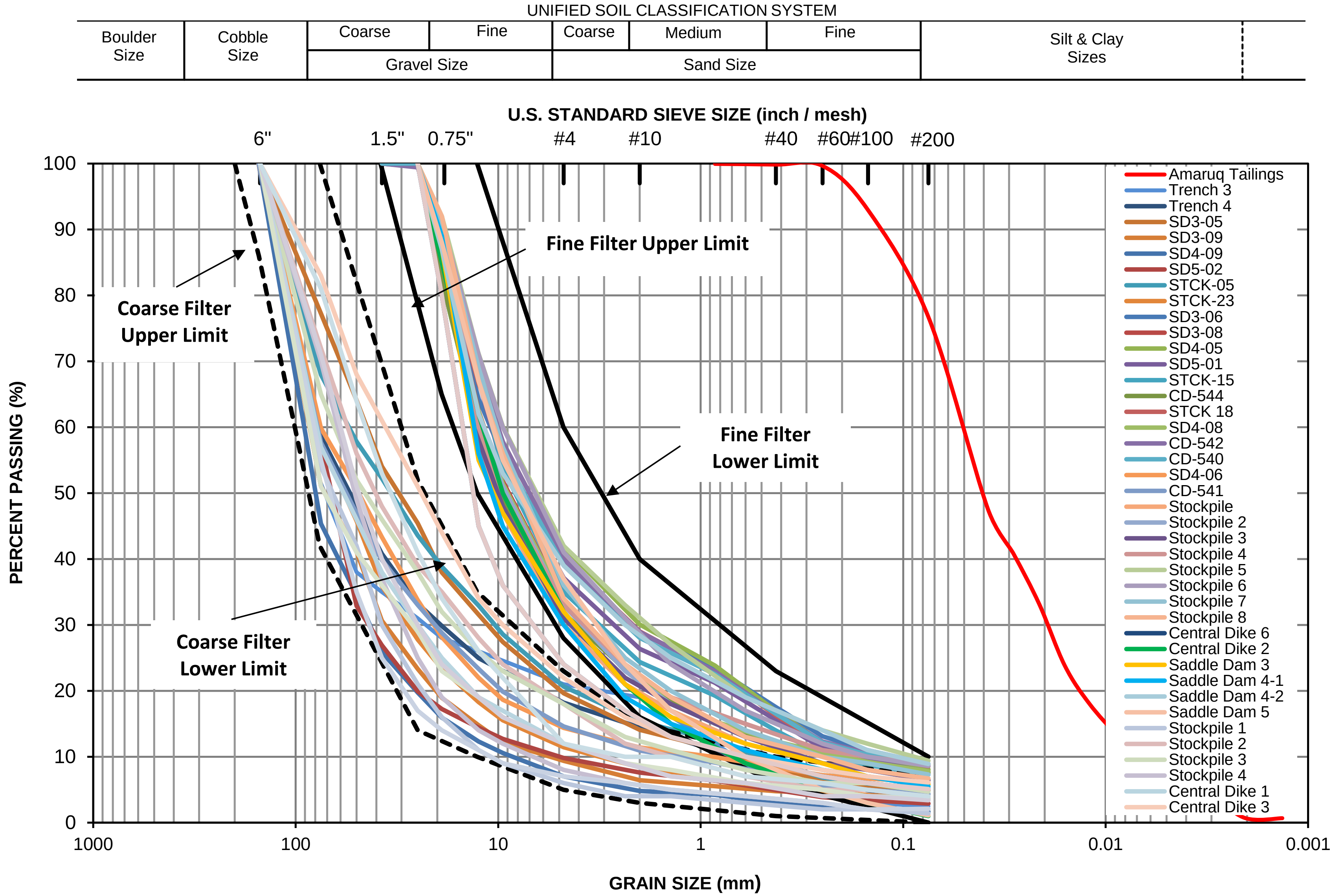

CLIENT **AEM**	PROJECT **Meadowbank North Cell TSF Design**

CONSULTANT

Golder Associates

YYYY-MM-DD	2016-05-27
DESIGNED	KH
PREPARED	RM
REVIEWED	KH
APPROVED	KAB

TITLE

Tailings and crushed waste rock particle size distributions and limits of filters

TITLE	PHASE	REV	FIGURE
1784383		**0**	**2**

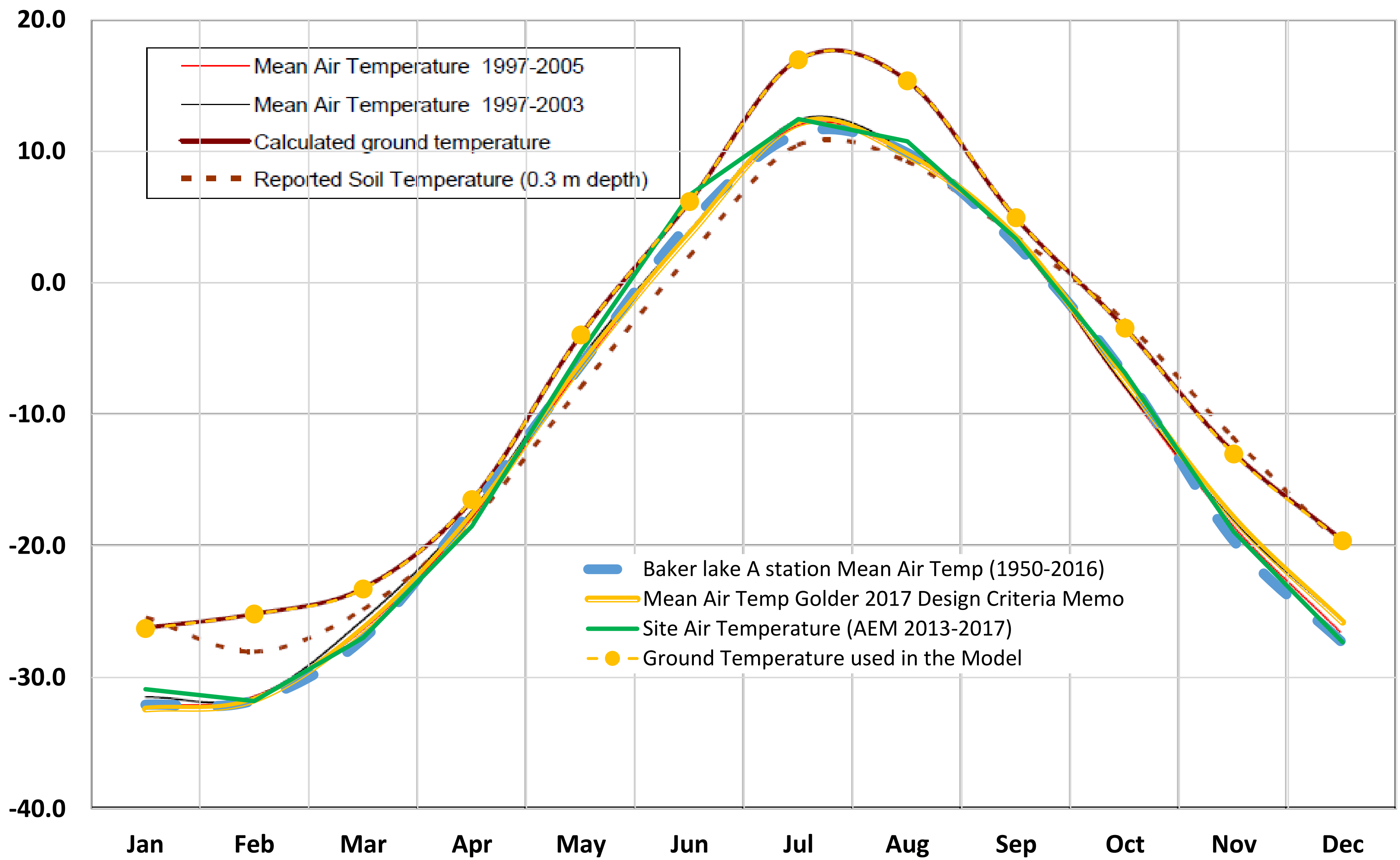

CLIENT **AEM**	PROJECT **Meadowbank North Cell TSF Design**

CONSULTANT

Golder Associates

YYYY-MM-DD	2016-05-27
DESIGNED	RM
PREPARED	RM
REVIEWED	FJ
APPROVED	KAB

TITLE

Ground Temperature Function

TITLE	PHASE	REV	FIGURE
1784383		**0**	**3**

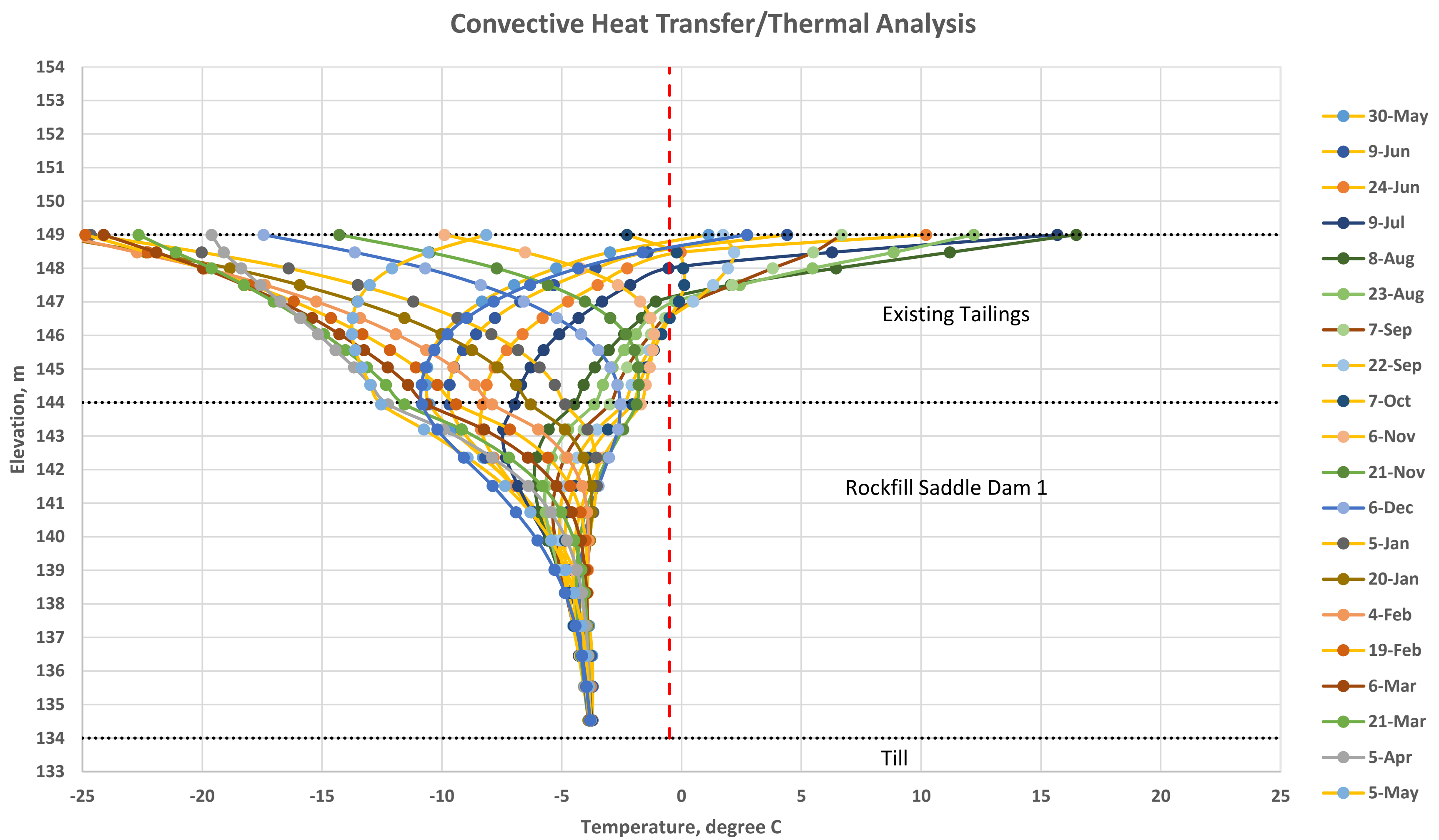

CLIENT
AEM

PROJECT
Meadowbank North Cell TSF Design

CONSULTANT

Golder Associates

YYYY-MM-DD	2017-12-15
DESIGNED	RM
PREPARED	RM
REVIEWED	FJ
APPROVED	KAB

TITLE
Variation of active zone depth at the toe of Cross-section 1

TITLE	PHASE	REV	FIGURE
1784383		**0**	**4**

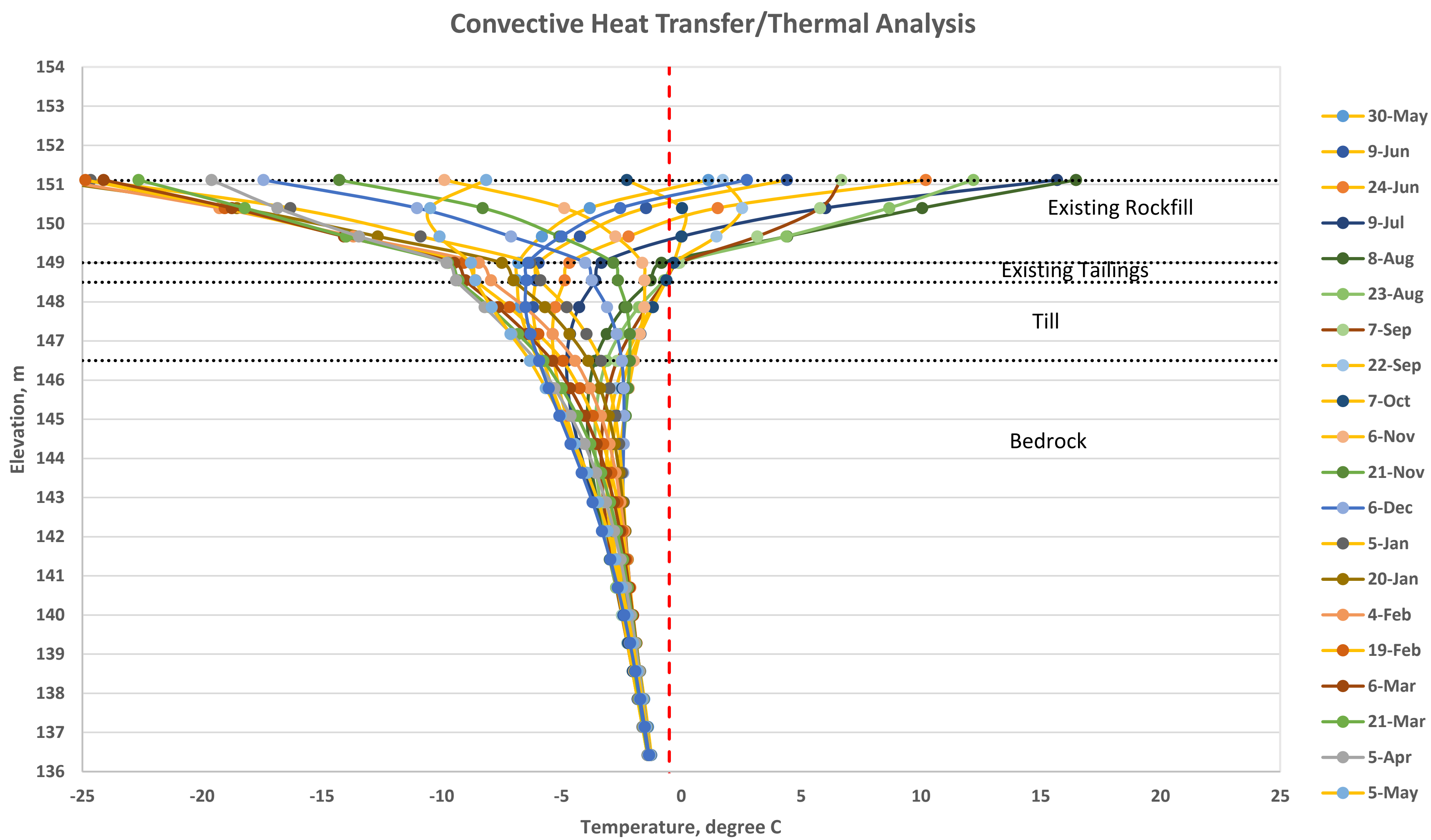

CLIENT **AEM**			PROJECT **Meadowbank North Cell TSF Design**
CONSULTANT Golder Associates	YYYY-MM-DD	2017-12-15	TITLE
	DESIGNED	RM	**Variation of active zone depth at the toe of Cross-section 2**
	PREPARED	RM	
	REVIEWED	FJ	TITLE **1784383** · PHASE · REV **0** · FIGURE **5**
	APPROVED	KAB	

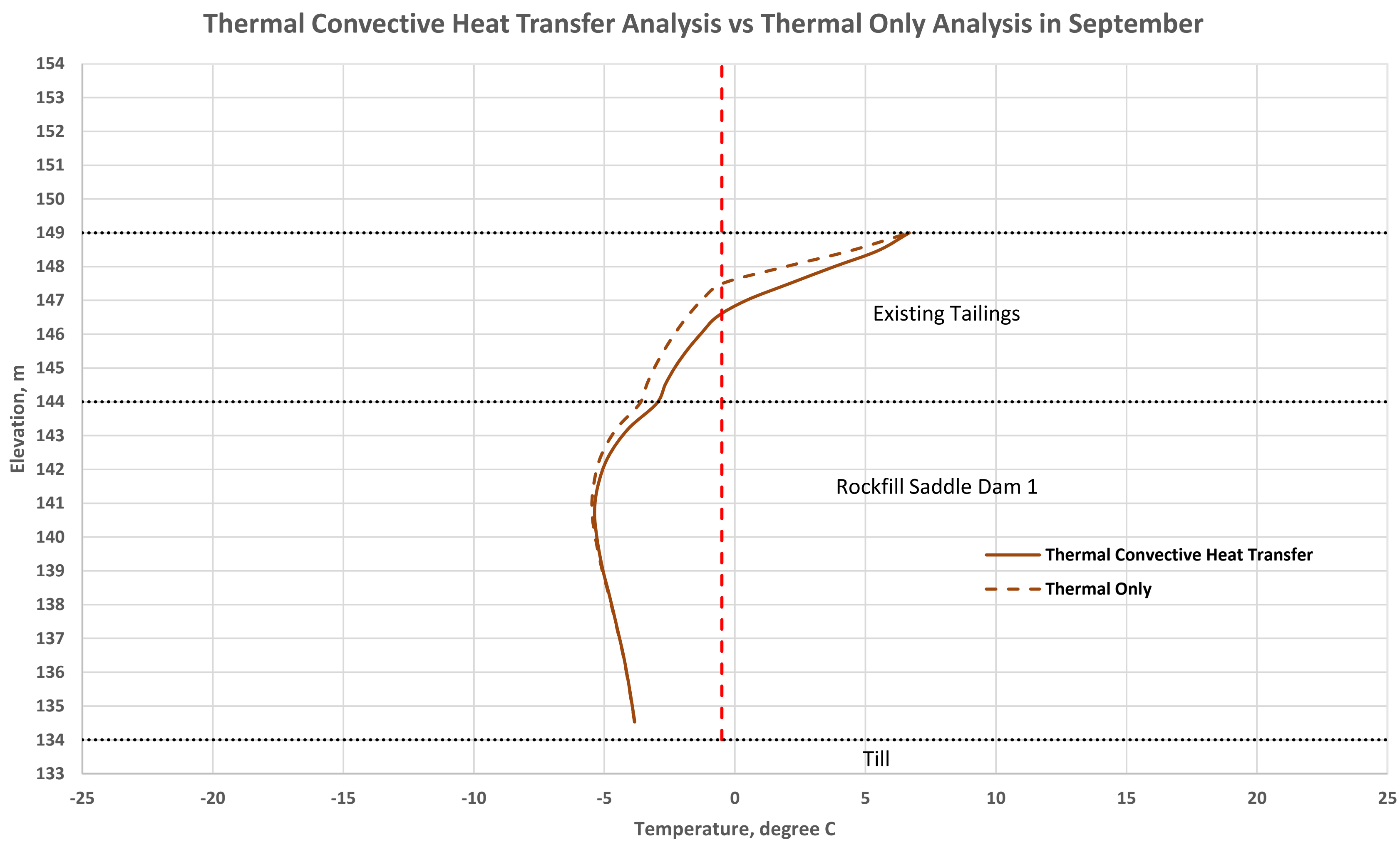

CLIENT **AEM**		PROJECT **Meadowbank North Cell TSF Design**	
CONSULTANT	YYYY-MM-DD	2017-12-15	TITLE **Comparsion between Thermal and Convective Heat Transfer Analyses for Cross-section 1**
Golder Associates	DESIGNED	RM	
	PREPARED	RM	
	REVIEWED	FJ	TITLE: **1784383** PHASE: REV: **0** FIGURE: **6**
	APPROVED	KAB	

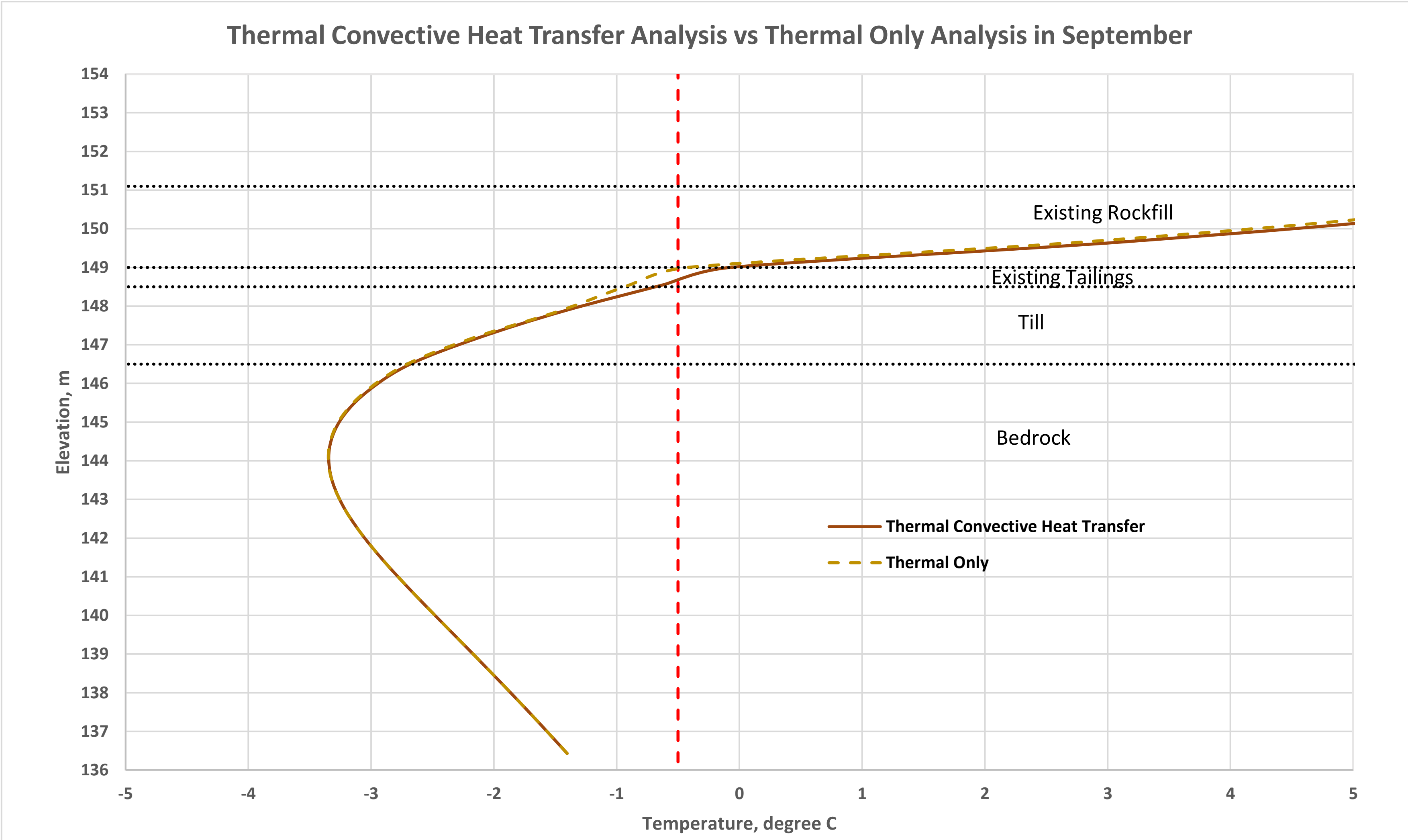

CLIENT **AEM**		PROJECT **Meadowbank North Cell TSF Design**	
CONSULTANT	YYYY-MM-DD: 2017-12-15	TITLE **Comparsion between Thermal and Convective Heat Transfer Analyses for Cross-section 2**	
Golder Associates	DESIGNED: RM		
	PREPARED: RM		
	REVIEWED: FJ	TITLE: **1784383** PHASE:	REV: **0** FIGURE: **7**
	APPROVED: KAB		

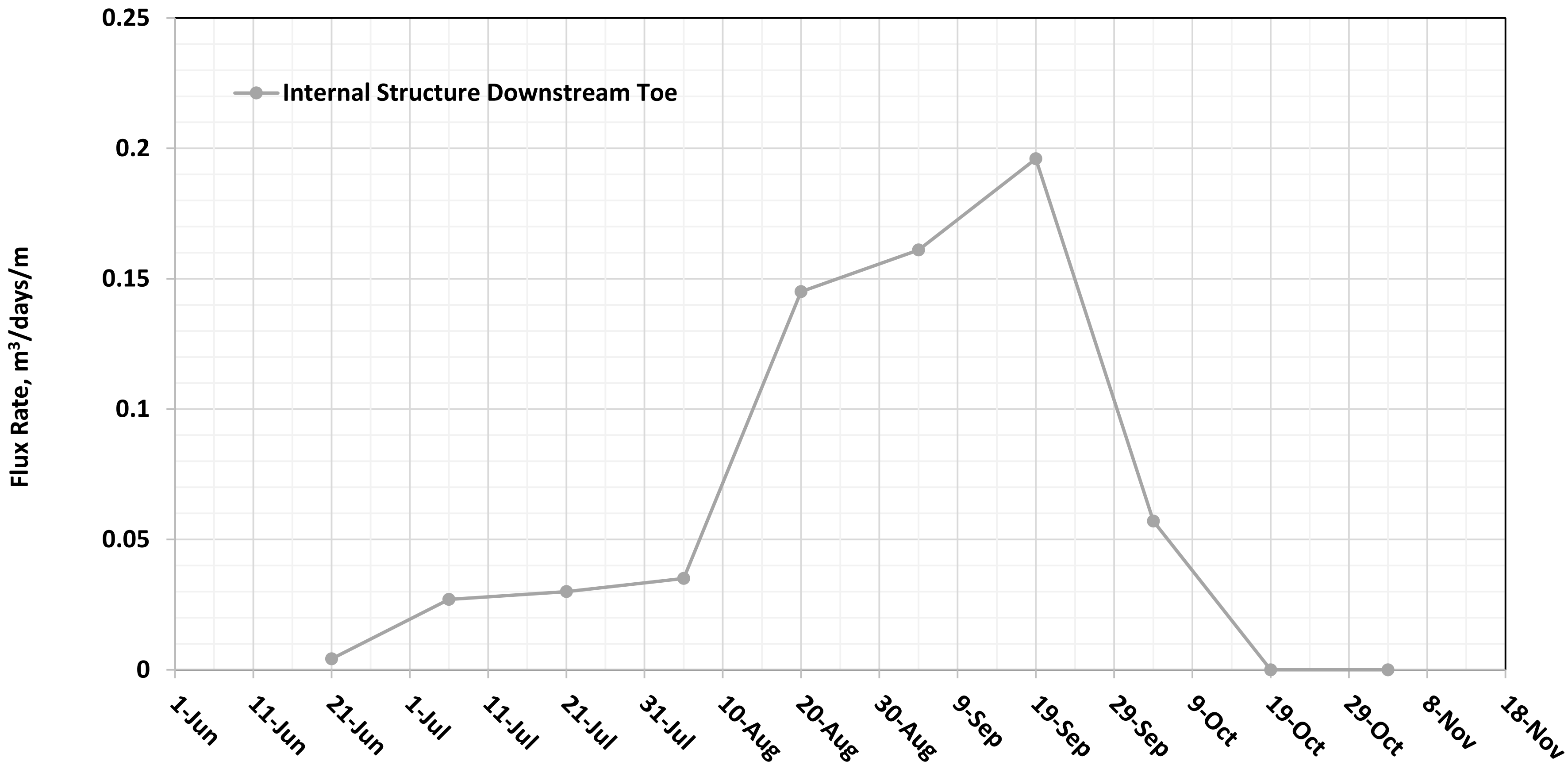

CLIENT **AEM**		PROJECT **Meadowbank North Cell TSF Design**	
CONSULTANT	YYYY-MM-DD	2017-12-15	TITLE
Golder Associates	DESIGNED	RM	**Variation of Flux Rate for Cross-section 1**
	PREPARED	RM	
	REVIEWED	FJ	TITLE / PHASE / REV / FIGURE
	APPROVED	KAB	**1784383** / / **0** / **8**

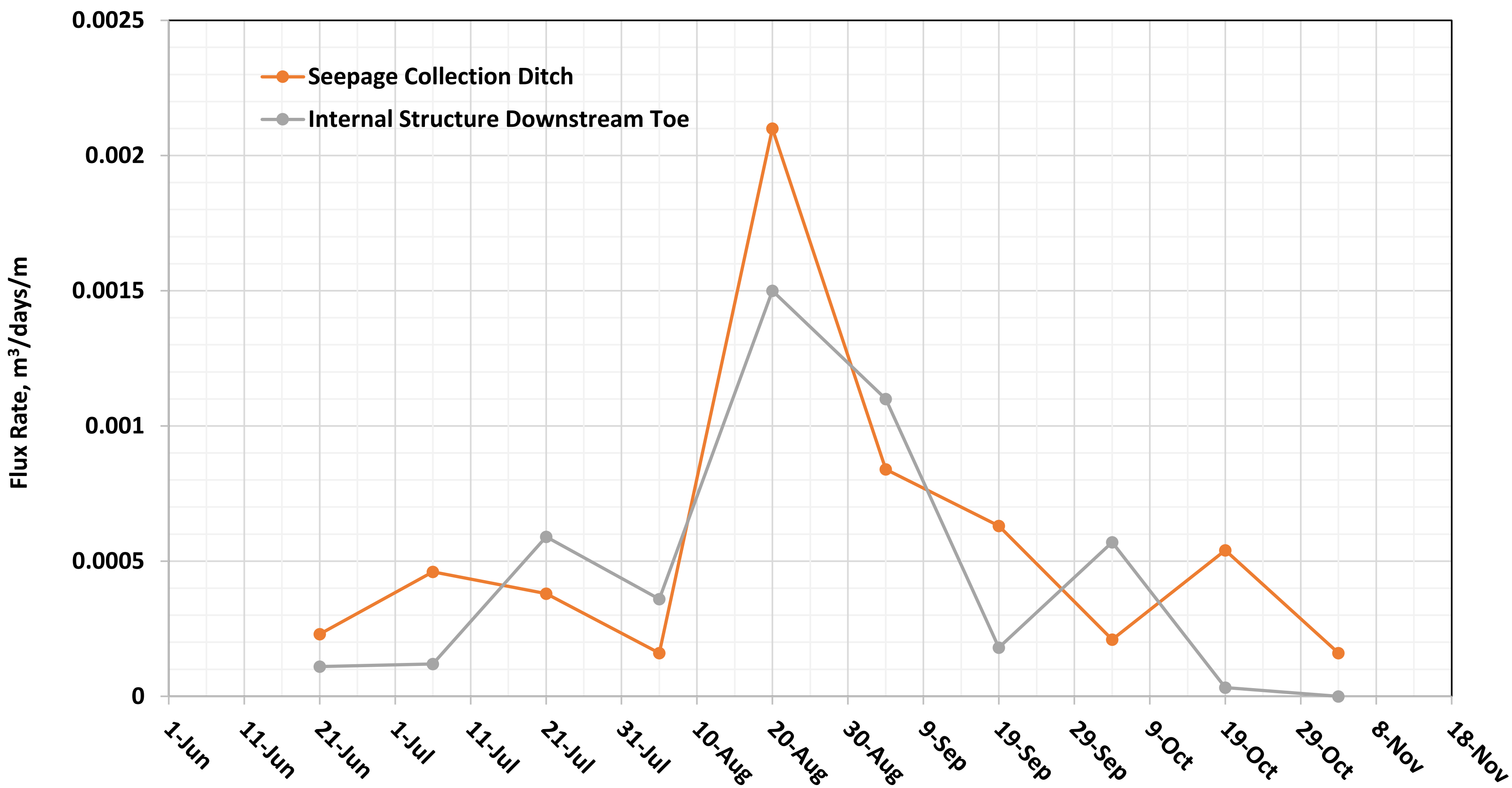

CLIENT **AEM**	PROJECT **Meadowbank North Cell TSF Design**

CONSULTANT

Golder Associates

YYYY-MM-DD	2017-12-15
DESIGNED	RM
PREPARED	RM
REVIEWED	FJ
APPROVED	KAB

TITLE

Variation of Flux Rate for Cross-section 2

TITLE	PHASE	REV	FIGURE
1784383		**0**	**9**

APPENDIX A

Construction Drawings